

A Partially Separable Temporal Model for Dynamic Valued Networks

Yik Lun Kei¹, Yanzhen Chen², and Oscar Hernan Madrid Padilla¹

¹Department of Statistics, University of California, Los Angeles

²Department of ISOM, Hong Kong University of Science and Technology

November 14, 2022

Abstract

The Exponential-family Random Graph Model (ERGM) is a powerful statistical model to represent the complicated structural dependencies of a binary network observed at a single time point. However, regarding dynamic valued networks whose observations are matrices of counts that evolve over time, the development of the ERGM framework is still in its infancy. We propose a Partially Separable Temporal ERGM (PST ERGM) for dynamic valued networks to facilitate the modeling of dyad value augmentation and dyad value diminution. Our parameter learning algorithms inherit state-of-the-art estimation techniques to approximate the maximum likelihood, by drawing Markov chain Monte Carlo (MCMC) samples conditioning on the network from the previous time step. We demonstrate the ability of the proposed model to interpret network dynamics and forecast temporal trends with real data.

Keywords: Temporal Exponential-family Random Graph Model; Temporal Weighted Networks; Markov chain Monte Carlo; Maximum Likelihood Estimation

1 Introduction

Networks are used to represent relational phenomena in many domains, such as human interaction in behavioral science (Eagle et al., 2006), gene regulation in cell biology (Wang et al., 2021), and scene graphs in computer vision (Suhail et al., 2021). Conventionally, a relation between two actors is indicated by the presence or absence of a tie: a binary state between two nodes in a network. Though connected ties are seemingly identical in binary networks, relations by nature often have degrees of strength, which can be represented by generic values to distinguish them. Transitioning from the dichotomous state of relation to the granular magnitude of strength requires a class of models to comprehend the richness of valued networks.

Established by Holland and Leinhardt (1981), Frank and Strauss (1986), and Wasserman and Pattison (1996), the Exponential-family Random Graph Model (ERGM) provides a flexible yet parsimonious way of modeling and simulating networks with complex structural patterns. As a

probability distribution of networks with dependent ties, ERGM defines local forces that shape global structure to facilitate statistical inference (Hunter et al., 2008b). Often, valued networks are dichotomized into binary networks for ERGM analysis. As polarization of dyad values conceals the quantitative information that original networks convey, Krivitsky (2012), Desmarais and Cranmer (2012), and Caimo and Gollini (2020) generalized the ERGM framework for modeling valued networks to prevent potential bias from data thresholding (Thomas and Blitzstein, 2011).

Relational phenomena also progress in time. For instance, Vanhems et al. (2013) investigated the transmission of hospital-acquired infections through recurring contacts among patients and health care workers. Similarly, as the volatile market of clean energy develops, Zhang et al. (2019) analyzed the syndicated investments under cooperating and competitive relations among venture capital firms. It is of great importance to understand when and how participants and their relations in a system change gradually. Robins and Pattison (2001) first studied the network dynamics over discrete time steps under the ERGM framework. Wyatt et al. (2009) and Wyatt et al. (2010) explicitly specified a dynamic feature term in ERGM to capture the change in dyad values over time. Hanneke and Xing (2006), and Hanneke et al. (2010) defined a Temporal ERGM (TERGM) to fit dynamic networks, by directly specifying a conditional ERGM between consecutive networks.

In recent decades, a plethora of discussions has concentrated on the modeling of dynamic networks. Donnat and Holmes (2018) provided a detailed guideline to characterize the structural change as networks progress. Jiang et al. (2020), and Goyal and De Gruttola (2020) pointed out that many frameworks only model snapshots of networks, which gives little prediction power in how future networks will evolve. Furthermore, Lerner et al. (2013), and Leifeld and Cranmer (2019) investigated the theoretical differences between the TERGM and the Stochastic Actor-Oriented Model, which is another popular framework developed by Snijders (2001) for dynamic network analysis. Other temporal networks models include Snijders (2005), Cranmer and Desmarais (2011), Sewell and Chen (2016), Rastelli et al. (2018), Ludkin et al. (2018), and Pensky (2019). With the attention to parameter interpretation that has been raised in the literature, a meticulous decomposition of network evolution as in Krivitsky and Handcock (2014) is needed to promote a realistic model for dynamic networks with both dyadic and temporal dependences.

For binary networks, network evolution regards (1) incidence: how often new ties are formed, and (2) duration: how long old ties last once they are formed. As shown in Krivitsky and Handcock (2014), these two factors can be positively and negatively associated at the same time, hence making the interpretation of models used in the literature problematic. Specifically, incidence and duration can be measured by dyad formation and dissolution, respectively. Posing that the process that results in dyad formation is different from the process that results in dyad dissolution, Krivitsky and Handcock (2014) proposed the Separable Temporal ERGM (STERGM) to dissect the confounding effects with two conditionally independent models for dynamic binary networks.

In this paper, we make the following contributions.

- We propose a Partially Separable Temporal ERGM (PST ERGM) to fit dynamic networks with counts dyad values, by assuming the underlying process that increases relational strength is different from the process that decreases relational strength. As we will demonstrate below, although our proposed model is no longer fully separable as the sample space of valued networks are infinite, the dynamics between consecutive networks are decomposed into two intermediate networks, where one controls dyad value augmentation and the other controls dyad value diminution. Our model specifies each transition with two sets of network statis-

tics derived from the intermediate networks and uses two distinct parameters to facilitate model interpretation.

- To align with the assumption that the two processes are usually unrelated but their models are not conditionally independent, we conduct approximate maximum likelihood estimation to collectively learn the parameters of the two processes. Since ERGM fitting is computationally intensive and sensitive to a poor initialization, we adapt the partial stepping and normality approximation for a static binary network from [Hummel et al. \(2012\)](#) to seed an adequate initialized configuration for learning PST ERGM of dynamic valued networks. Subsequently, we employ the Newton-Raphson method from [Hanneke et al. \(2010\)](#) to refine the parameters of the augmentation and diminution processes. Throughout we exploit the Contrastive Divergence sampling, an abridged MCMC from [Hummel \(2011\)](#) and [Krivitsky \(2017\)](#), to speed up the sampling procedure.
- Our experiments show a good performance of the proposed model and algorithms. In particular, a time-heterogeneous PST ERGM on the students contact data ([Mastrandrea et al., 2015](#)) provides a realistic interpretation of the network dynamics. Furthermore, a time-homogeneous PST ERGM on the baboons interaction data ([Gelardi et al., 2020](#)) produces reasonable out-of-sample forecasts of the temporal trends.

The rest of the paper is organized as follows. In Section 2, we review ERGM frameworks for static binary networks, static valued networks, and dynamic binary networks. In Section 3, we propose the PST ERGM to fit dynamic valued networks, with specifications on the intermediate networks. In Section 4, we provide algorithms for the approximate maximum likelihood estimation and the Metropolis-Hastings algorithm for drawing dynamic valued networks. In Section 5, we illustrate the methodology with simulated and real data examples.

2 ERGM for Networks

2.1 Background on Static Binary and Valued Networks

For a fixed set $N = \{1, 2, \dots, n\}$ of nodes, we can use a network $\mathbf{y} \in \mathcal{Y}$, in the form of an $n \times n$ matrix, to represent the potential relations for all pairs $(i, j) \in \mathbb{Y} \subseteq N \times N$. The binary networks have dyad $\mathbf{y}_{ij} \in \{0, 1\}$ to represent the absence or presence of a tie and $\mathcal{Y} \subseteq 2^{\mathbb{Y}}$. Let \mathbb{N}_0 be the set of natural numbers and 0. The valued networks have dyad $\mathbf{y}_{ij} \in \mathbb{N}_0$ to represent the intensity of a tie and $\mathcal{Y} \subseteq \mathbb{N}_0^{\mathbb{Y}}$. We disallow a network to have self-edge, so $\mathbf{y}_{ij} = 0$ if $i = j$. The relation in a network can be either directed or undirected, where undirected network has $\mathbf{y}_{ij} = \mathbf{y}_{ji}$ for all dyads (i, j) .

The probabilistic formulation of an ERGM for a network \mathbf{y} is

$$P(\mathbf{y}; \boldsymbol{\eta}) = h(\mathbf{y}) \exp[\boldsymbol{\eta}^\top \mathbf{g}(\mathbf{y}) - \psi(\boldsymbol{\eta})]$$

where $\mathbf{g}(\mathbf{y})$, with $\mathbf{g} : \mathcal{Y} \rightarrow \mathbb{R}^p$, is a vector of network statistics; $\boldsymbol{\eta} \in \mathbb{R}^p$ is a vector of unknown parameters; $\exp[\psi(\boldsymbol{\eta})] = \sum_{\mathbf{y} \in \mathcal{Y}} h(\mathbf{y}) \exp[\boldsymbol{\eta}^\top \mathbf{g}(\mathbf{y})]$ is the normalizing constant; $h(\mathbf{y})$, with $h : \mathcal{Y} \rightarrow [0, \infty)$, is the reference function. The network statistics $\mathbf{g}(\mathbf{y})$ may also depend on nodal

attributes \mathbf{x} such as the gender of participants and edge attributes \mathbf{e} such as the type of relationships. For notational simplicity, we omit the dependence of $\mathbf{g}(\mathbf{y})$ on \mathbf{x} and \mathbf{e} as they are implicitly included.

Network statistics $\mathbf{g}(\mathbf{y})$ that describe an $n \times n$ network with only p numeric summaries play a central role in the ERGM framework. A representative ERGM for an observed network \mathbf{y}^{obs} has sufficient statistics $\mathbf{g}(\mathbf{y}^{\text{obs}})$ that capture its significant features well. These features can signify the underlying process that originally produces the observed network. In addition, as a probability distribution of networks, ERGM allows us to sample various $n \times n$ networks that share similar network statistics as $\mathbf{g}(\mathbf{y}^{\text{obs}})$, by using a careful design of the Metropolis-Hastings algorithm. [Handcock et al. \(2021\)](#), an R library for social network analysis, provides a comprehensive list of network statistics.

Given a single observed network \mathbf{y}^{obs} in ERGM fitting, the maximum likelihood estimator (MLE)

$$\hat{\boldsymbol{\eta}} = \arg \max_{\boldsymbol{\eta}} \log[h(\mathbf{y}^{\text{obs}})] + \boldsymbol{\eta}^\top \mathbf{g}(\mathbf{y}^{\text{obs}}) - \log\left\{\sum_{\mathbf{y} \in \mathcal{Y}} h(\mathbf{y}) \exp[\boldsymbol{\eta}^\top \mathbf{g}(\mathbf{y})]\right\}$$

satisfies

$$\mathbf{S}(\boldsymbol{\eta}) = \mathbf{g}(\mathbf{y}^{\text{obs}}) - \mathbb{E}_{\boldsymbol{\eta}}[\mathbf{g}(\mathbf{y})] = \mathbf{0}$$

where $\mathbf{S}(\boldsymbol{\eta})$ is the gradient of log-likelihood with respect to $\boldsymbol{\eta}$ and $\mathbb{E}_{\boldsymbol{\eta}}[\mathbf{g}(\mathbf{y})]$ denotes the expectation of network statistics under the distribution $P(\mathbf{y}; \boldsymbol{\eta})$. The gradient $\mathbf{S}(\boldsymbol{\eta})$ is driven by the difference between the observed network statistics $\mathbf{g}(\mathbf{y}^{\text{obs}})$ and the expected network statistics $\mathbb{E}_{\boldsymbol{\eta}}[\mathbf{g}(\mathbf{y})]$. The latter can be estimated by sampling networks from $P(\mathbf{y}; \boldsymbol{\eta})$. In this context, the chosen network statistics serve as constraints to the sample space \mathcal{Y} , since ERGM fitting is essentially a feature pursuit: finding a parameter $\boldsymbol{\eta}$ such that its expected network statistics are not different from the observed network statistics.

In valued ERGM, the parameter space of $\boldsymbol{\eta}$ has to ensure that $P(\mathbf{y}; \boldsymbol{\eta})$ is a valid distribution. As in [Krivitsky \(2012\)](#), when the range of values for each dyad in a network is $\{0\} \cup \mathbb{N}$, the condition $\exp[\psi(\boldsymbol{\eta})] < \infty$ is sufficient to guarantee that $P(\mathbf{y}; \boldsymbol{\eta})$ is a valid distribution. Furthermore, the reference function $h(\mathbf{y})$ underlies a baseline distribution of dyad values. That is when $\boldsymbol{\eta} = \mathbf{0}$, $P(\mathbf{y}; \boldsymbol{\eta}) \propto h(\mathbf{y})$. [Krivitsky \(2012\)](#) defined a Poisson-reference ERGM and [Krivitsky \(2019\)](#) defined a Binomial-reference ERGM for valued networks with respective reference functions:

$$h_{\text{Pois}}(\mathbf{y}) = \prod_{(i,j) \in \mathbb{Y}} (\mathbf{y}_{ij}!)^{-1} \quad \text{and} \quad h_{\text{Bino}}(\mathbf{y}) = \prod_{(i,j) \in \mathbb{Y}} \binom{m}{\mathbf{y}_{ij}}$$

where m is a known maximum value that each relationship $\mathbf{y}_{ij} \in \{0, 1, \dots, m\}$ can take in this network. For binary ERGM, usually $h(\mathbf{y}) = 1$ (e.g., [Wasserman and Pattison, 1996](#); [Snijders, 2002](#); [Snijders et al., 2006](#); [Hunter and Handcock, 2006](#)).

2.2 Background on Dynamic Binary Networks

The Temporal ERGM (TERGM) from [Hanneke et al. \(2010\)](#) for a binary network \mathbf{y}^t conditional on \mathbf{y}^{t-1} is

$$P(\mathbf{y}^t | \mathbf{y}^{t-1}; \boldsymbol{\eta}) = \exp[\boldsymbol{\eta}^\top \mathbf{g}(\mathbf{y}^t | \mathbf{y}^{t-1}) - \psi(\boldsymbol{\eta} | \mathbf{y}^{t-1})]$$

where $\mathbf{y}^t \in \mathcal{Y}^t$ is a single network at a discrete time point t and $\mathbf{g}(\mathbf{y}^t|\mathbf{y}^{t-1})$, with $\mathbf{g} : \mathcal{Y}^t \times \mathcal{Y}^{t-1} \rightarrow \mathbb{R}^p$, is a vector of network statistics for the transition from \mathbf{y}^{t-1} to \mathbf{y}^t . Yet models neglecting the confounding effect of incidence and duration can lead to misinterpretation of the underlying process that produces the networks. Krivitsky and Handcock (2014) demonstrated a contrasting interpretation of a TERGM parameter, which emphasized the importance of careful decomposition of network dynamics. Given two consecutive binary networks \mathbf{y}^{t-1} and \mathbf{y}^t , a TERGM with a higher coefficient on the count of ties

$$\mathbf{g}(\mathbf{y}^t|\mathbf{y}^{t-1}) = \sum_{(i,j) \in \mathbb{Y}} \mathbf{y}_{ij}^t$$

would favor networks with more ties at time t . The increment of this network statistic can be achieved in two ways concurrently: previously empty dyads will start to form ties at time t , and previously existing ties will remain at time t . Both incidence and duration are increased. On the contrary, a TERGM with a higher coefficient on the measure of stability

$$\mathbf{g}(\mathbf{y}^t|\mathbf{y}^{t-1}) = \frac{1}{n-1} \sum_{(i,j) \in \mathbb{Y}} [\mathbf{y}_{ij}^t \mathbf{y}_{ij}^{t-1} + (1 - \mathbf{y}_{ij}^t)(1 - \mathbf{y}_{ij}^{t-1})]$$

would favor networks that do not change much at time t . The constancy of this network statistic is achieved by not forming ties on previously empty dyads and by not dissolving previously existing ties simultaneously. In this case, the incidence is decreased but duration is increased. Therefore, a higher coefficient in TERGM can lead to inconsistent interpretation of network evolution.

Krivitsky and Handcock (2014) proposed the Separable Temporal ERGM (STERGM) to dissect the comprehension of network evolution. The incidence, how often new ties are formed, can be measured by dyad formation $\mathbf{y}_{ij}^{t-1} = 0 \rightarrow \mathbf{y}_{ij}^t = 1$. The duration, how long old ties last, can be traced by dyad dissolution $\mathbf{y}_{ij}^{t-1} = 1 \rightarrow \mathbf{y}_{ij}^t = 0$. Instead of directly modeling the observed \mathbf{y}^{t-1} and \mathbf{y}^t that muddle parameter interpretation, we can construct two intermediate networks, formation network $\mathbf{y}^{+,t}$ and dissolution network $\mathbf{y}^{-,t}$, between time $t-1$ and time t to reflect incidence and duration. Particularly, the formation network $\mathbf{y}^{+,t} \in \mathcal{Y}^{+,t}$ is acquired by adding the edges formed at time t to \mathbf{y}^{t-1} so $\mathcal{Y}^{+,t} \subseteq \{\mathbf{y} \in 2^{\mathbb{Y}} : \mathbf{y} \supseteq \mathbf{y}^{t-1}\}$. The dissolution network $\mathbf{y}^{-,t} \in \mathcal{Y}^{-,t}$ is acquired by removing the edges dissolved at time t from \mathbf{y}^{t-1} so $\mathcal{Y}^{-,t} \subseteq \{\mathbf{y} \in 2^{\mathbb{Y}} : \mathbf{y} \subseteq \mathbf{y}^{t-1}\}$. Table 1 gives all four possible transitions of a binary dyad $\mathbf{y}_{ij} \in \{0, 1\}$ between two consecutive time steps and their corresponding constructed $\mathbf{y}_{ij}^{+,t}$ and $\mathbf{y}_{ij}^{-,t}$.

$\mathbf{y}_{ij}^{t-1} \rightarrow \mathbf{y}_{ij}^t$	$\mathbf{y}_{ij}^{+,t}$	$\mathbf{y}_{ij}^{-,t}$
0 \rightarrow 0	0	0
0 \rightarrow 1	1	0
1 \rightarrow 0	1	0
1 \rightarrow 1	1	1

Table 1: Possible transition and construction of formation and dissolution networks for a binary dyad.

Subsequently, as $\mathbf{y}^{+,t}$ is conditionally independent of $\mathbf{y}^{-,t}$ given \mathbf{y}^{t-1} , the STERGM for \mathbf{y}^t conditional on \mathbf{y}^{t-1} is

$$P(\mathbf{y}^t|\mathbf{y}^{t-1}; \boldsymbol{\eta}^+, \boldsymbol{\eta}^-) = P(\mathbf{y}^{+,t}|\mathbf{y}^{t-1}; \boldsymbol{\eta}^+) \times P(\mathbf{y}^{-,t}|\mathbf{y}^{t-1}; \boldsymbol{\eta}^-) \quad (1)$$

where

$$\begin{aligned} P(\mathbf{y}^{+,t}|\mathbf{y}^{t-1};\boldsymbol{\eta}^+) &= \exp[\boldsymbol{\eta}^+ \cdot \mathbf{g}^+(\mathbf{y}^{+,t}|\mathbf{y}^{t-1}) - \psi(\boldsymbol{\eta}^+|\mathbf{y}^{t-1})], \\ P(\mathbf{y}^{-,t}|\mathbf{y}^{t-1};\boldsymbol{\eta}^-) &= \exp[\boldsymbol{\eta}^- \cdot \mathbf{g}^-(\mathbf{y}^{-,t}|\mathbf{y}^{t-1}) - \psi(\boldsymbol{\eta}^-|\mathbf{y}^{t-1})]. \end{aligned}$$

The intuition behind the separable parameterization of STERGM is that the factors and processes that result in ties formation are different from those that result in ties dissolution. Many applications of STERGM on real-world data support the separable assumption for dynamic network analysis (e.g., Broekel and Bednarz, 2018; Uppala and Handcock, 2020; Xie et al., 2020; Deng et al., 2021). In contrast to the TERGM whose parameters simultaneously influence both incidence and duration, STERGM provides two sets of parameters, where one manages ties formation and the other manages ties dissolution. Furthermore, in accordance with the separable assumption, a distinct choice of $\mathbf{g}^-(\mathbf{y}^{-,t}|\mathbf{y}^{t-1})$ from $\mathbf{g}^+(\mathbf{y}^{+,t}|\mathbf{y}^{t-1})$ based on user’s analysis is allowed to facilitate a realistic dynamic network model. Despite the restriction that the two processes do not interact with each other, substantial improvement in interpretability is gained.

3 Temporal ERGM for Valued Networks

3.1 Augmentation and Diminution Networks

As relational phenomena evolve over time, it is assumed that the factors and underlying processes that increase relational strength are different from those that decrease relational strength. For instance, in an intensive care unit of a hospital, the number of contacts between a doctor and a patient increases as the doctor frequently treats the patient during the early stage of infection, and it escalates when the patient’s symptoms worsen. In contrast, the number of contacts decreases as the patient acquires immunity to the disease, and it plummets as the doctor uses medical sensors to monitor the patient after the symptoms alleviate. In alignment with the motivation of STERGM, network evolution for valued networks where $\mathbf{y}_{ij}^{t-1}, \mathbf{y}_{ij}^t \in \{0\} \cup \mathbb{N}$ also concerns incidence and duration.

However, we need to broaden the scope of incidence and duration by encoding the fluctuations of dyad values to develop a realistic model for dynamic valued networks. We regard incidence as how often dyad values increase, and we encode incidence with how much dyad values at time t have increased. Likewise, we regard duration as how long dyad values have kept increasing until they start to decrease, and we encode duration with how much dyad values at time t have decreased. In this setting, the incidence can be measured by dyad value augmentation $\mathbf{y}_{ij}^t \geq \mathbf{y}_{ij}^{t-1}$. The duration can be traced by dyad value diminution $\mathbf{y}_{ij}^t \leq \mathbf{y}_{ij}^{t-1}$, since the duration of increment is the inverse of the rate at which dyad values decrease. Next, we will define two intermediate networks to reflect the above dynamics.

Given two consecutive valued networks \mathbf{y}^{t-1} and \mathbf{y}^t , we can construct the augmentation network $\mathbf{y}^{+,t}$ and the diminution network $\mathbf{y}^{-,t}$ between time $t-1$ and time t for dyad (i, j) as follows:

$$\begin{aligned} \mathbf{y}_{ij}^{+,t} &= f^+(\mathbf{y}_{ij}^{t-1}, \mathbf{y}_{ij}^t) = \max(\mathbf{y}_{ij}^{t-1}, \mathbf{y}_{ij}^t), \\ \mathbf{y}_{ij}^{-,t} &= f^-(\mathbf{y}_{ij}^{t-1}, \mathbf{y}_{ij}^t) = \min(\mathbf{y}_{ij}^{t-1}, \mathbf{y}_{ij}^t). \end{aligned} \tag{2}$$

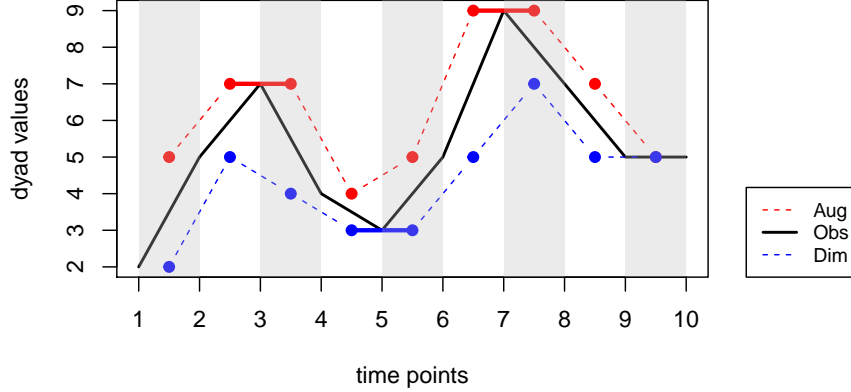


Figure 1: Construction of augmentation (Aug) and diminution (Dim) networks for a particular dyad.

These are also generalized formulations of the formation network $\mathbf{y}^{+,t}$ and the dissolution network $\mathbf{y}^{-,t}$ in Krivitsky and Handcock (2014), since binary networks are special cases of valued networks in terms of dyad values. In summary, $\mathbf{y}^{+,t}$ contains the unchanged dyad values from time $t-1$ to time t and those that increased at time t , while $\mathbf{y}^{-,t}$ contains the unchanged dyad values from time $t-1$ to time t and those that decreased at time t . Furthermore, both of them preserve the momentum when the dyad value starts to change in the opposite direction. As the bolded segments shown in Figure 1, the momentum of the changes is delayed to the next interval for a model to digest the stimulus. Alternatively, $\mathbf{y}^{+,t}$ and $\mathbf{y}^{-,t}$ can be considered as latent networks that emphasize the transitions between time $t-1$ and time t , instead of two snapshots of the observed networks \mathbf{y}^t and \mathbf{y}^{t-1} .

3.2 Model Specification

We first define the form of the model for a sequence of valued networks $\mathbf{y}^1, \dots, \mathbf{y}^T$, with ERGM specified as the transitions between consecutive networks. Under the first order Markov assumption where \mathbf{y}^t is independent of $\mathbf{y}^{t-2}, \dots, \mathbf{y}^1$ conditioning on \mathbf{y}^{t-1} , we have

$$\begin{aligned} P(\mathbf{y}^T, \mathbf{y}^{T-1}, \dots, \mathbf{y}^2 | \mathbf{y}^1) &= P(\mathbf{y}^T | \mathbf{y}^{T-1}) P(\mathbf{y}^{T-1} | \mathbf{y}^{T-2}) \dots P(\mathbf{y}^2 | \mathbf{y}^1) \\ &= \prod_{t=2}^T h(\mathbf{y}^t | \mathbf{y}^{t-1}) \exp[\boldsymbol{\eta} \cdot \mathbf{g}(\mathbf{y}^t | \mathbf{y}^{t-1}) - \psi(\boldsymbol{\eta} | \mathbf{y}^{t-1})]. \end{aligned}$$

Besides the dynamics between consecutive networks, $P(\mathbf{y}^1)$ can be specified by a valued ERGM (Krivitsky, 2012).

To dissect the entanglement between incidence and duration in dynamic valued networks, it may be straightforward to consider that the augmentation network $\mathbf{y}^{+,t}$ is also conditionally independent of the diminution network $\mathbf{y}^{-,t}$ given \mathbf{y}^{t-1} , as in the STERGM for dynamic binary networks. However, as we will compare the two cases below, a separable model for dynamic valued networks can be difficult to obtain, while retaining the information encoded in $\mathbf{y}^{+,t}$ and $\mathbf{y}^{-,t}$ of Equation (2).

For dynamic binary networks where $\mathcal{Y}^t \subseteq 2^{\mathbb{Y}}$, the STERGM of Equation (1) as a generative model permits us to sample $\mathbf{y}^{+,t}$ and $\mathbf{y}^{-,t}$ individually to produce a unique $\mathbf{y}^t \in \mathcal{Y}^t$. Conditioning on \mathbf{y}^{t-1} with a particular dyad $\mathbf{y}_{ij}^{t-1} = 0$, the sampled $\mathbf{y}_{ij}^{-,t}$ can only be 0 whereas the sampled $\mathbf{y}_{ij}^{+,t}$ can be either 0 or 1. Once $\mathbf{y}_{ij}^{+,t}$ is determined, a unique \mathbf{y}_{ij}^t is confirmed. Similarly, conditioning on \mathbf{y}^{t-1} with a particular dyad $\mathbf{y}_{ij}^{t-1} = 1$, $\mathbf{y}_{ij}^{+,t}$ can only be 1 whereas $\mathbf{y}_{ij}^{-,t}$ can be either 0 or 1. Once $\mathbf{y}_{ij}^{-,t}$ is determined, a unique \mathbf{y}_{ij}^t is confirmed. Therefore, a separable model in the spaces of $\mathcal{Y}^{+,t}$ and $\mathcal{Y}^{-,t}$ proposed by Krivitsky and Handcock (2014) is a valid probability distribution for a binary network $\mathbf{y}^t \in \mathcal{Y}^t$ conditional on \mathbf{y}^{t-1} .

For dynamic valued networks where $\mathcal{Y}^t \subseteq \mathbb{N}_0^{\mathbb{Y}}$, suppose $P(\mathbf{y}^t|\mathbf{y}^{t-1})$ can still be separated into two conditionally independent models as in Equation (1), so that we can sample $\mathbf{y}^{+,t}$ and $\mathbf{y}^{-,t}$ individually to produce a unique $\mathbf{y}^t \in \mathcal{Y}^t$. Conditioning on \mathbf{y}^{t-1} with a particular dyad value $\mathbf{y}_{ij}^{t-1} \in \mathbb{N}_0$ and under the specification of Equation (2), a sampled $\mathbf{y}_{ij}^{-,t}$ can be any non-negative count value that is smaller than or equal to \mathbf{y}_{ij}^{t-1} , and a sampled $\mathbf{y}_{ij}^{+,t}$ can be any count value that is greater than or equal to \mathbf{y}_{ij}^{t-1} . For instance, conditioning on \mathbf{y}^{t-1} with a particular dyad value $\mathbf{y}_{ij}^{t-1} = 3$ and sampling $\mathbf{y}^{+,t}$ and $\mathbf{y}^{-,t}$ to generate \mathbf{y}^t as in Equation (1), when the sampled $\mathbf{y}_{ij}^{-,t}$ from $P(\mathbf{y}^{-,t}|\mathbf{y}^{t-1}; \boldsymbol{\eta}^-)$ is 2 and the sampled $\mathbf{y}_{ij}^{+,t}$ from $P(\mathbf{y}^{+,t}|\mathbf{y}^{t-1}; \boldsymbol{\eta}^+)$ is 5, a unique \mathbf{y}_{ij}^t is unidentifiable given the two intermediate dyad values. The separated generating processes cannot decide whether the dyad value $\mathbf{y}_{ij}^{t-1} = 3$ has increased to $\mathbf{y}_{ij}^t = 5$ or decreased to $\mathbf{y}_{ij}^t = 2$.

Since the TERGM in our framework can no longer be separated into two conditionally independent models as in Krivitsky and Handcock (2014), our proposed Partially Separable Temporal ERGM (PST ERGM) for a sequence of valued networks is

$$\begin{aligned} \prod_{t=2}^T P(\mathbf{y}^t|\mathbf{y}^{t-1}; \boldsymbol{\eta}) &= \prod_{t=2}^T h(\mathbf{y}^t|\mathbf{y}^{t-1}) \exp[\boldsymbol{\eta} \cdot \mathbf{g}(\mathbf{y}^t|\mathbf{y}^{t-1}) - \psi(\boldsymbol{\eta}|\mathbf{y}^{t-1})] \\ &= \prod_{t=2}^T h^+(\mathbf{y}^{+,t}) h^-(\mathbf{y}^{-,t}) \frac{\exp[\boldsymbol{\eta}^+ \cdot \mathbf{g}^+(\mathbf{y}^{+,t}|\mathbf{y}^{t-1}) + \boldsymbol{\eta}^- \cdot \mathbf{g}^-(\mathbf{y}^{-,t}|\mathbf{y}^{t-1})]}{\exp[\psi(\boldsymbol{\eta}^+, \boldsymbol{\eta}^-|\mathbf{y}^{t-1})]} \end{aligned} \quad (3)$$

with $\boldsymbol{\eta} = (\boldsymbol{\eta}^+, \boldsymbol{\eta}^-)$, $\mathbf{g}(\mathbf{y}^t|\mathbf{y}^{t-1}) = [\mathbf{g}^+(\mathbf{y}^{+,t}|\mathbf{y}^{t-1}), \mathbf{g}^-(\mathbf{y}^{-,t}|\mathbf{y}^{t-1})]$, $h(\mathbf{y}^t|\mathbf{y}^{t-1}) = h^+(\mathbf{y}^{+,t}) \times h^-(\mathbf{y}^{-,t})$, and the normalizing constant $\exp[\psi(\boldsymbol{\eta}|\mathbf{y}^{t-1})]$ is

$$\sum_{\mathbf{y}^t \in \mathcal{Y}^t} h^+(\mathbf{y}^{+,t}) \exp[\boldsymbol{\eta}^+ \cdot \mathbf{g}^+(\mathbf{y}^{+,t}|\mathbf{y}^{t-1})] \times h^-(\mathbf{y}^{-,t}) \exp[\boldsymbol{\eta}^- \cdot \mathbf{g}^-(\mathbf{y}^{-,t}|\mathbf{y}^{t-1})].$$

In this article, we also use the Poisson and Binomial reference functions:

$$h^+(\mathbf{y}^{+,t}) = \prod_{(i,j) \in \mathbb{Y}} (\mathbf{y}_{ij}^{+,t}!)^{-1} \quad \text{and} \quad h^-(\mathbf{y}^{-,t}) = \prod_{(i,j) \in \mathbb{Y}} \binom{m}{\mathbf{y}_{ij}^{-,t}}$$

for the augmentation and diminution process respectively. The term m in $h^-(\mathbf{y}^{-,t})$ is a pre-determined maximum value that each dyad value $\mathbf{y}_{ij}^{-,t} \in \{0, 1, \dots, m\}$ can take in $\mathbf{y}^{-,t}$, and it is fixed across $t = 2, \dots, T$. To underlie the baseline distribution, the reference function $h^+(\mathbf{y}^{+,t})$ in the augmentation process does not require an upper bound for a dyad value $\mathbf{y}_{ij}^{+,t}$ that it can increase to, but $\mathbf{y}_{ij}^{+,t}$ has an implicit lower bound that is equal to \mathbf{y}_{ij}^{t-1} inherited from the construction of $\mathbf{y}_{ij}^{+,t} = \max(\mathbf{y}_{ij}^{t-1}, \mathbf{y}_{ij}^t)$. In the diminution process, the reference function $h^-(\mathbf{y}^{-,t})$ imposes an

upper bound m for each dyad value $\mathbf{y}_{ij}^{-,t}$ that it can decrease from, with an explicit lower bound that is equal to 0.

In practice, the structural property of a network changes as it evolves over time. To capture the variation between different intervals, we can also specify a time-heterogeneous PST ERGM $\prod_{t=2}^T P(\mathbf{y}^t | \mathbf{y}^{t-1}; \boldsymbol{\eta}^t)$ as

$$\prod_{t=2}^T \frac{h^+(\mathbf{y}^{+,t}) \exp[\boldsymbol{\eta}^{+,t} \cdot \mathbf{g}^+(\mathbf{y}^{+,t} | \mathbf{y}^{t-1})] \times h^-(\mathbf{y}^{-,t}) \exp[\boldsymbol{\eta}^{-,t} \cdot \mathbf{g}^-(\mathbf{y}^{-,t} | \mathbf{y}^{t-1})]}{\exp[\psi(\boldsymbol{\eta}^{+,t}, \boldsymbol{\eta}^{-,t} | \mathbf{y}^{t-1})]}$$

where parameter $\boldsymbol{\eta}^t = (\boldsymbol{\eta}^{+,t}, \boldsymbol{\eta}^{-,t})$ differs by time t . Furthermore, we let the term m in $h^-(\mathbf{y}^{-,t})$ be varied by t , and m^t is chosen to be the maximum dyad values of $\mathbf{y}^{-,t}$ that is constructed from the observed \mathbf{y}^{t-1} and observed \mathbf{y}^t . Unless otherwise noted, we focus on the time-homogeneous PST ERGM of Equation (3) whose parameter $\boldsymbol{\eta} = (\boldsymbol{\eta}^+, \boldsymbol{\eta}^-)$ is fixed across $t = 2, \dots, T$. The time-heterogeneous PST ERGM is a special case of Equation (3) as the parameter $\boldsymbol{\eta}^t = (\boldsymbol{\eta}^{+,t}, \boldsymbol{\eta}^{-,t})$ is learned sequentially for each t .

Our proposed PST ERGM for dynamic valued networks

$$P(\mathbf{y}^t | \mathbf{y}^{t-1}) \propto \exp[\boldsymbol{\eta}^+ \cdot \mathbf{g}^+(\mathbf{y}^{+,t} | \mathbf{y}^{t-1})] \times \exp[\boldsymbol{\eta}^- \cdot \mathbf{g}^-(\mathbf{y}^{-,t} | \mathbf{y}^{t-1})]$$

is partially separable, and the STERGM for dynamic binary networks given as

$$P(\mathbf{y}^t | \mathbf{y}^{t-1}) = \frac{\exp[\boldsymbol{\eta}^+ \cdot \mathbf{g}^+(\mathbf{y}^{+,t} | \mathbf{y}^{t-1})]}{\exp[\psi(\boldsymbol{\eta}^+ | \mathbf{y}^{t-1})]} \times \frac{\exp[\boldsymbol{\eta}^- \cdot \mathbf{g}^-(\mathbf{y}^{-,t} | \mathbf{y}^{t-1})]}{\exp[\psi(\boldsymbol{\eta}^- | \mathbf{y}^{t-1})]}$$

(Krivitsky and Handcock, 2014) is fully separable. The idea of separability is originated from epidemiology to approximate disease dynamics: Prevalence \approx Incidence \times Duration. Translating this into network evolution, the structural property of dynamic valued networks is a characterization of the amount and rate of dyad values augmentation and diminution. In general, for a particular positive $\mathbf{g}_i^+(\mathbf{y}^{+,t} | \mathbf{y}^{t-1})$ in the augmentation process, a positive $\boldsymbol{\eta}_i^+$ is associated with increasing dyad values to have more instances of the feature that is tracked by $\mathbf{g}_i^+(\mathbf{y}^{+,t} | \mathbf{y}^{t-1})$ in $\mathbf{y}^{+,t}$. On the contrary, a negative $\boldsymbol{\eta}_i^+$ will disrupt the emergence of this feature by not increasing dyad values, resulting in fewer instances of the feature. For a particular positive $\mathbf{g}_i^-(\mathbf{y}^{-,t} | \mathbf{y}^{t-1})$ in the diminution process, a positive $\boldsymbol{\eta}_i^-$ is associated with not decreasing dyad values to preserve more instances of the feature that is tracked by $\mathbf{g}_i^-(\mathbf{y}^{-,t} | \mathbf{y}^{t-1})$. However, a negative $\boldsymbol{\eta}_i^-$ will target this feature by reducing dyad values, resulting in fewer instances of the feature. Equivalently, a negative $\boldsymbol{\eta}_i^-$ is also associated with a shorter duration of the feature appearance.

Figure 2 gives an overview of the PST ERGM for dynamic valued networks. The white solid circles denote the observed networks $\mathbf{y}^1, \dots, \mathbf{y}^T$ as time passes from left to right. The dashed circles on the top denote the sequence of augmentation networks $\mathbf{y}^{+,t}$ and the dotted circles on the bottom denote the sequence of diminution networks $\mathbf{y}^{-,t}$ for $t = 2, \dots, T$. The intermediate networks in both sequences are recovered from the observed networks with Equation (2) between consecutive time steps. The model with respect to the observed networks is partially separated into the augmentation process and the diminution process. Once the parameters in the triangle nodes are learned collectively, we can perform MCMC sampling to generate a future network $\hat{\mathbf{y}}^{T+1}$ in the forecasting process. Though \mathbf{y}^t can be further conditioned on more previous networks to calculate the network statistics and to construct $\mathbf{y}^{+,t}$ and $\mathbf{y}^{-,t}$ in Equation (2), we only discuss the PST ERGM with first order Markov assumption in this article.

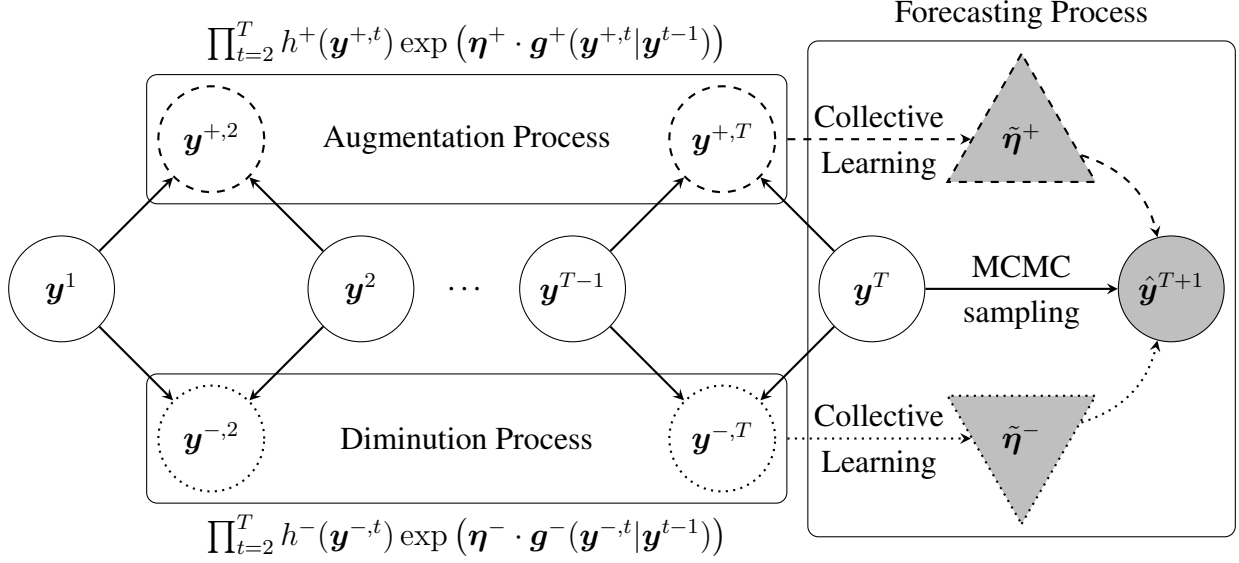


Figure 2: An illustration of PST ERGM for dynamic valued networks.

4 Likelihood-Based Inference

4.1 Log-likelihood Ratio

The log-likelihood of $P(\mathbf{y}^T, \mathbf{y}^{T-1}, \dots, \mathbf{y}^2 | \mathbf{y}^1; \boldsymbol{\eta}) = \prod_{t=2}^T P(\mathbf{y}^t | \mathbf{y}^{t-1}; \boldsymbol{\eta})$ is

$$l(\boldsymbol{\eta}) = \sum_{t=2}^T \left\{ \log[h(\mathbf{y}^t | \mathbf{y}^{t-1})] + \boldsymbol{\eta} \cdot \mathbf{g}(\mathbf{y}^t | \mathbf{y}^{t-1}) - \psi(\boldsymbol{\eta} | \mathbf{y}^{t-1}) \right\}. \quad (4)$$

The term $\exp[\psi(\boldsymbol{\eta} | \mathbf{y}^{t-1})]$ involves a sum over all possible networks in $\mathcal{Y}^t \subseteq \mathbb{N}_0^{\mathbb{Y}}$, which is often computationally intractable except for special cases such as small networks (Yon et al., 2021) or models with particular conditional independence properties (Lauritzen et al., 2018). Consequently, we approximate the MLE using MCMC methods. To maximize the log-likelihood, we calculate its first and second derivative with respect to $\boldsymbol{\eta}$:

$$\mathbf{S}(\boldsymbol{\eta}) = \sum_{t=2}^T \left\{ \mathbf{g}(\mathbf{y}^t | \mathbf{y}^{t-1}) - \mathbb{E}_{\boldsymbol{\eta}}[\mathbf{g}(\mathbf{y}^t | \mathbf{y}^{t-1})] \right\} \quad \text{and} \quad \mathbf{H}(\boldsymbol{\eta}) = \sum_{t=2}^T -\text{Cov}[\mathbf{g}(\mathbf{y}^t | \mathbf{y}^{t-1})] \quad (5)$$

where $\mathbb{E}_{\boldsymbol{\eta}}[\mathbf{g}(\mathbf{y}^t | \mathbf{y}^{t-1})]$ denotes the expectation of network statistics and $\text{Cov}[\mathbf{g}(\mathbf{y}^t | \mathbf{y}^{t-1})]$ denotes the covariance of network statistics, both with respect to the distribution $P(\mathbf{y}^t | \mathbf{y}^{t-1}; \boldsymbol{\eta})$. Approximating $\mathbb{E}_{\boldsymbol{\eta}}[\mathbf{g}(\mathbf{y}^t | \mathbf{y}^{t-1})]$ and $\text{Cov}[\mathbf{g}(\mathbf{y}^t | \mathbf{y}^{t-1})]$ with MCMC samples, the parameter $\boldsymbol{\eta}$ can be updated iteratively by Newton-Raphson method. However, it is computationally expensive to generate new MCMC samples at each iteration of parameter update.

To reduce the computational burden of MCMC sampling, we can use the log-likelihood ratio as a new objective function to approximate the MLE as in Hunter and Handcock (2006). Let $\boldsymbol{\eta}_0$ be another initialized parameter, the log-likelihood ratio is

$$r(\boldsymbol{\eta}, \boldsymbol{\eta}_0) = \sum_{t=2}^T \left\{ (\boldsymbol{\eta} - \boldsymbol{\eta}_0)^\top \mathbf{g}(\mathbf{y}^t | \mathbf{y}^{t-1}) - \log \left\{ \exp[\psi(\boldsymbol{\eta} | \mathbf{y}^{t-1})] - \exp[\psi(\boldsymbol{\eta}_0 | \mathbf{y}^{t-1})] \right\} \right\}$$

and the ratio of two normalizing constants at time step t satisfies

$$\frac{\exp[\psi(\boldsymbol{\eta}|\mathbf{y}^{t-1})]}{\exp[\psi(\boldsymbol{\eta}_0|\mathbf{y}^{t-1})]} = \mathbb{E}_{\boldsymbol{\eta}_0} \left\{ \exp[(\boldsymbol{\eta} - \boldsymbol{\eta}_0)^\top \mathbf{g}(\mathbf{y}^t|\mathbf{y}^{t-1})] \right\}.$$

Note that the distribution to draw samples from is now changed as we introduce an initialized parameter $\boldsymbol{\eta}_0$ to the log-likelihood ratio.

Generating a sufficiently large number of samples from $P(\mathbf{y}^t|\mathbf{y}^{t-1}; \boldsymbol{\eta}_0)$ only once for each time t , and then iterating a Newton-Raphson method with respect to $\boldsymbol{\eta}$ until convergence yields a maximizer of the approximated log-likelihood ratio. Though anchored on pre-determined samples that are drawn from $P(\mathbf{y}^t|\mathbf{y}^{t-1}; \boldsymbol{\eta}_0)$ can greatly expedite the estimation process, the efficiency of not having to update the MCMC samples between learning iterations of $\boldsymbol{\eta}$ comes with a cost. [Geyer and Thompson \(1992\)](#) pointed out that the approximated log-likelihood ratio via MCMC samples degrades quickly as $\boldsymbol{\eta}_0$ moves away from $\boldsymbol{\eta}$, so the parameter estimation in the above setting is highly sensitive to the initialization of $\boldsymbol{\eta}_0$. [Krivitsky \(2017\)](#) also emphasized the importance of a good initial configuration in ERGM fitting, as a poor starting point can lead to non-convergence of parameter learning algorithms. We address these issues in the next subsection.

4.2 Normality Approximation and Partial Stepping

[Hummel et al. \(2012\)](#) proposed two amendments to improve the approximation of the log-likelihood ratio for a static binary network. We adapt them to the PST ERGM of dynamic valued networks to seed an initial starting point, followed by the Newton-Raphson method to further refine the parameter. Let $\mathbf{y}_1^t, \dots, \mathbf{y}_s^t$ be a list of s networks sampled from $P(\mathbf{y}^t|\mathbf{y}^{t-1}; \boldsymbol{\eta}_0)$. Since they are drawn from the same distribution, we can assume their network statistics multiplied by the difference of the two parameters, $(\boldsymbol{\eta} - \boldsymbol{\eta}_0)^\top \mathbf{g}(\mathbf{y}^t|\mathbf{y}^{t-1})$, follow a normal distribution $\mathcal{N}(\mu_t, \sigma_t^2)$ with

$$\mu_t = (\boldsymbol{\eta} - \boldsymbol{\eta}_0)^\top \boldsymbol{\mu}_t \quad \text{and} \quad \sigma_t^2 = (\boldsymbol{\eta} - \boldsymbol{\eta}_0)^\top \boldsymbol{\Sigma}_t (\boldsymbol{\eta} - \boldsymbol{\eta}_0)$$

where $\boldsymbol{\mu}_t$ and $\boldsymbol{\Sigma}_t$ are the respective mean vector and covariance matrix of $\mathbf{g}(\mathbf{y}^t|\mathbf{y}^{t-1})$ evaluated from the sampled networks $\mathbf{y}_1^t, \dots, \mathbf{y}_s^t$. Given that $\exp[(\boldsymbol{\eta} - \boldsymbol{\eta}_0)^\top \mathbf{g}(\mathbf{y}^t|\mathbf{y}^{t-1})]$ is now log-normally distributed, the ratio of the two normalizing constants can be replaced by

$$\exp[\psi(\boldsymbol{\eta}|\mathbf{y}^{t-1}) - \psi(\boldsymbol{\eta}_0|\mathbf{y}^{t-1})] = \mathbb{E}_{\boldsymbol{\eta}_0} \left\{ \exp[(\boldsymbol{\eta} - \boldsymbol{\eta}_0)^\top \mathbf{g}(\mathbf{y}^t|\mathbf{y}^{t-1})] \right\} = \exp(\mu_t + \frac{1}{2}\sigma_t^2)$$

and the approximated log-likelihood ratio becomes

$$\hat{r}_s(\boldsymbol{\eta}, \boldsymbol{\eta}_0) = (\boldsymbol{\eta} - \boldsymbol{\eta}_0)^\top \left[\sum_{t=2}^T \mathbf{g}(\mathbf{y}^t|\mathbf{y}^{t-1}) - \sum_{t=2}^T \boldsymbol{\mu}_t \right] - \frac{1}{2} (\boldsymbol{\eta} - \boldsymbol{\eta}_0)^\top \left[\sum_{t=2}^T \boldsymbol{\Sigma}_t \right] (\boldsymbol{\eta} - \boldsymbol{\eta}_0).$$

Although the approximated log-likelihood ratio $\hat{r}_s(\boldsymbol{\eta}, \boldsymbol{\eta}_0)$ degrades quickly as $\boldsymbol{\eta}_0$ moves away from $\boldsymbol{\eta}$, we can restrict the amount of parameter update to prevent the degradation of $\hat{r}_s(\boldsymbol{\eta}, \boldsymbol{\eta}_0)$. With a step length $\gamma \in (0, 1]$, we create a pseudo-observation

$$\hat{\boldsymbol{\xi}}(\mathbf{y}) = \gamma \sum_{t=2}^T \mathbf{g}(\mathbf{y}^t|\mathbf{y}^{t-1}) + (1 - \gamma) \sum_{t=2}^T \boldsymbol{\mu}_t \quad (6)$$

in between the observed network statistics $\sum_{t=2}^T \mathbf{g}(\mathbf{y}^t | \mathbf{y}^{t-1})$ and the current estimated network statistics $\sum_{t=2}^T \boldsymbol{\mu}_t$ from MCMC samples that are drawn from $P(\mathbf{y}^t | \mathbf{y}^{t-1}; \boldsymbol{\eta}_0)$. Recall that ERGM fitting is driven by the difference between observed and expected network statistics. Instead of the difference between $\sum_{t=2}^T \boldsymbol{\mu}_t$ and $\sum_{t=2}^T \mathbf{g}(\mathbf{y}^t | \mathbf{y}^{t-1})$, we learn the parameter based on the difference between $\sum_{t=2}^T \boldsymbol{\mu}_t$ and the pseudo-observation $\hat{\boldsymbol{\xi}}(\mathbf{y})$ in each learning iteration to limit the amount of parameter update.

Thus, we sequentially update the parameter in the direction of the MLE, while maintaining that the approximated log-likelihood ratio $\hat{r}_s(\boldsymbol{\eta}, \boldsymbol{\eta}_0)$ estimated by MCMC samples is reasonably accurate within each learning iteration. Combining the normality approximation and partial stepping, the closed-form solution for the maximizer of the approximated log-likelihood ratio at a specific learning iteration is

$$\begin{aligned} \tilde{\boldsymbol{\eta}} &= \arg \max_{\boldsymbol{\eta}} (\boldsymbol{\eta} - \boldsymbol{\eta}_0)^\top [\hat{\boldsymbol{\xi}}(\mathbf{y}) - \sum_{t=2}^T \boldsymbol{\mu}_t] - \frac{1}{2} (\boldsymbol{\eta} - \boldsymbol{\eta}_0)^\top \left[\sum_{t=2}^T \boldsymbol{\Sigma}_t \right] (\boldsymbol{\eta} - \boldsymbol{\eta}_0) \\ &= \boldsymbol{\eta}_0 + \left[\sum_{t=2}^T \boldsymbol{\Sigma}_t \right]^{-1} [\hat{\boldsymbol{\xi}}(\mathbf{y}) - \sum_{t=2}^T \boldsymbol{\mu}_t]. \end{aligned}$$

Once a parameter is obtained from maximizing the approximated log-likelihood ratio with the above setting, we proceed to the Newton-Raphson method to further update the parameter near its convergence. In this fusion where each component performs its designated task, both procedures require shorter learning iterations and undertake smaller computational burdens than only on their own.

4.3 MCMC for Networks

Fitting PST ERGM and forecasting networks can be heavily dependent on MCMC sampling. In this subsection, we introduce the Metropolis-Hastings algorithm for drawing \mathbf{y}^t conditional on \mathbf{y}^{t-1} . The superscript t is omitted for \mathbf{y}^t , $\mathbf{y}^{+,t}$ and $\mathbf{y}^{-,t}$ to facilitate notational simplicity, as MCMC sampling is performed within a particular time step t . Additionally, we use a superscript k to refer to the current MCMC iteration.

In practice, valued networks are often sparse. To accommodate the sparsity of networks, as our proposal distribution, we employ a zero-inflated Poisson distribution that is also used in [Krivitsky \(2019\)](#), an R library for static valued networks:

$$P(\mathbf{y}_{ij}^{k+1}; \lambda, \pi_0) = \begin{cases} \pi_0 + (1 - \pi_0) \exp(-\lambda) & \text{if } \mathbf{y}_{ij}^{k+1} = 0 \\ (1 - \pi_0) \exp(-\lambda) \times \lambda^{\mathbf{y}_{ij}^{k+1}} / \mathbf{y}_{ij}^{k+1}! & \text{if } \mathbf{y}_{ij}^{k+1} \in \mathbb{N} \end{cases} \quad (7)$$

where $\lambda = \mathbf{y}_{ij}^k + 0.5$ and $\pi_0 \in [0, 1)$ is a pre-defined probability for the proposed dyad jumping to 0. The 0.5 in λ prevents the proposed value \mathbf{y}_{ij}^{k+1} from locking into 0 when $\mathbf{y}_{ij}^k = 0$. In this work, we let $\pi_0 = 0.2$, a default value for the Poisson proposal distribution used in [Krivitsky \(2019\)](#) and it can be adjusted based on the user's prior knowledge on the sparsity of networks. The acceptance ratio α for the proposed dyad value \mathbf{y}_{ij}^{k+1} is

$$q \times \frac{\mathbf{y}_{ij}^{+,k!}}{\mathbf{y}_{ij}^{+,k+1}!} \exp[\boldsymbol{\eta}^+ \cdot \Delta \mathbf{g}^+(\mathbf{y}^+ | \mathbf{y}^{t-1})_{ij}] \times \binom{m}{\mathbf{y}_{ij}^{-,k+1}} / \binom{m}{\mathbf{y}_{ij}^{-,k}} \exp[\boldsymbol{\eta}^- \cdot \Delta \mathbf{g}^-(\mathbf{y}^- | \mathbf{y}^{t-1})_{ij}] \quad (8)$$

where \mathbf{y}^+ and \mathbf{y}^- are constructed accordingly from the observed \mathbf{y}^{t-1} and the proposed network at MCMC iteration $k + 1$. The change statistics $\Delta \mathbf{g}^+(\mathbf{y}^+|\mathbf{y}^{t-1})_{ij}$ denote the difference between $\mathbf{g}^+(\mathbf{y}^+|\mathbf{y}^{t-1})$ with $\mathbf{y}_{ij}^+ = \mathbf{y}_{ij}^{+,k+1}$ and $\mathbf{g}^+(\mathbf{y}^+|\mathbf{y}^{t-1})$ with $\mathbf{y}_{ij}^+ = \mathbf{y}_{ij}^{+,k}$, and the change statistics $\Delta \mathbf{g}^-(\mathbf{y}^-|\mathbf{y}^{t-1})_{ij}$ denote the difference between $\mathbf{g}^-(\mathbf{y}^-|\mathbf{y}^{t-1})$ with $\mathbf{y}_{ij}^- = \mathbf{y}_{ij}^{-,k+1}$ and $\mathbf{g}^-(\mathbf{y}^-|\mathbf{y}^{t-1})$ with $\mathbf{y}_{ij}^- = \mathbf{y}_{ij}^{-,k}$, while rest of the \mathbf{y}^+ and \mathbf{y}^- remain unchanged. Finally, the transition probability ratio q is

$$q = \frac{P(\mathbf{y}_{ij}^k; \lambda = \mathbf{y}_{ij}^{k+1} + 0.5, \pi_0)}{P(\mathbf{y}_{ij}^{k+1}; \lambda = \mathbf{y}_{ij}^k + 0.5, \pi_0)}.$$

In summary, we propose a dyad value from the space of \mathbf{y}^t , but we decide to accept the proposed dyad value based on the construction of augmentation network $\mathbf{y}^{+,t}$ and diminution network $\mathbf{y}^{-,t}$, namely the dynamics between time $t - 1$ and time t . As we consolidate the temporal aspect into the PST ERGM, MCMC sampling becomes especially important in forecasting future networks besides its primary usage in parameter learning. Conditioning on the last observed network \mathbf{y}^T under the first order Markov assumption, we can forecast $\hat{\mathbf{y}}^{T+1}$ given the learned parameters $\tilde{\eta}^+$ and $\tilde{\eta}^-$ with the above scheme.

4.4 Algorithms

The partial stepping algorithm of PST ERGM parameter estimation to seed an initial configuration is provided in Algorithm 1. See [Hummel et al. \(2012\)](#) for a detailed guideline on choosing the step length. In this work, we let γ_c be the ratio of the current iteration c to the maximum number of iterations C . Only in the last learning iteration where $\gamma_c = 1$ do we use the difference between observed network statistics $\sum_{t=2}^T \mathbf{g}(\mathbf{y}^t|\mathbf{y}^{t-1})$ and estimated network statistics $\sum_{t=2}^T \boldsymbol{\mu}_t$ to update the parameter. The Newton-Raphson algorithm of PST ERGM parameter estimation is provided in Algorithm 2.

Algorithm 1 Partial stepping algorithm

- 1: **Input:** initialized parameter $\boldsymbol{\eta}_0$, learning iteration C , sample size s , $\{\mathbf{y}^1, \dots, \mathbf{y}^T\}$
 - 2: **for** $c = 1, \dots, C$ **do**
 - 3: **for** $t = 2, \dots, T$ **do**
 - 4: Generate s MCMC samples $\mathbf{y}_1^t, \dots, \mathbf{y}_s^t$ from $P(\mathbf{y}^t|\mathbf{y}^{t-1}; \boldsymbol{\eta}_{c-1})$ as in Section 4.3
 - 5: Calculate mean vector $\boldsymbol{\mu}_t$ of $\{\mathbf{g}(\mathbf{y}_1^t|\mathbf{y}^{t-1}), \dots, \mathbf{g}(\mathbf{y}_s^t|\mathbf{y}^{t-1})\}$
 - 6: Calculate covariance matrix $\boldsymbol{\Sigma}_t$ of $\{\mathbf{g}(\mathbf{y}_1^t|\mathbf{y}^{t-1}), \dots, \mathbf{g}(\mathbf{y}_s^t|\mathbf{y}^{t-1})\}$
 - 7: **end for**
 - 8: For $\gamma_c = c/C$, calculate $\hat{\boldsymbol{\xi}}(\mathbf{y}) = \gamma_c \sum_{t=2}^T \mathbf{g}(\mathbf{y}^t|\mathbf{y}^{t-1}) + (1 - \gamma_c) \sum_{t=2}^T \boldsymbol{\mu}_t$
 - 9: $\boldsymbol{\eta}_c = \boldsymbol{\eta}_{c-1} + [\sum_{t=2}^T \boldsymbol{\Sigma}_t]^{-1} [\hat{\boldsymbol{\xi}}(\mathbf{y}) - \sum_{t=2}^T \boldsymbol{\mu}_t]$
 - 10: **end for**
 - 11: $\tilde{\boldsymbol{\eta}} \leftarrow \boldsymbol{\eta}_c$
 - 12: **Output:** learned parameter $\tilde{\boldsymbol{\eta}}$
-

[Hummel \(2011\)](#) applied a K -step Contrastive Divergence (CD_K) sampling, an abridged MCMC, to speed up parameter estimation. Introduced in [Hinton \(2002\)](#) and [Carreira-Perpinan and Hinton](#)

(2005) and applied to ERGM frameworks in [Fellows \(2014\)](#) and [Krivitsky \(2017\)](#), the Contrastive Divergence for ERGM is formulated as

$$\text{CD}_K = \text{KL}[P_{\text{data}}(\mathbf{y}^{\text{obs}}) \parallel P_{\infty}(\mathbf{y})] - \text{KL}[P_K(\mathbf{y}) \parallel P_{\infty}(\mathbf{y})]$$

where $P_{\text{data}}(\mathbf{y}^{\text{obs}})$ is the distribution of the observed data, $P_{\infty}(\mathbf{y})$ is the true model distribution, and $P_K(\mathbf{y})$ is the distribution of K -step MCMC samples. The gradient of CD_K for minimization that is given as

$$\nabla \text{CD}_K = \mathbf{g}(\mathbf{y}^{\text{obs}}) - \mathbb{E}_K[\mathbf{g}(\mathbf{y})] = \mathbf{0}$$

builds the foundation of CD_K sampling, where $\mathbb{E}_K[\mathbf{g}(\mathbf{y})]$ is the expected network statistics under the distribution of K -step MCMC samples.

Algorithm 2 Newton-Raphson algorithm

- 1: **Input:** initialized parameter η_0 , learning iteration C , sample size s , $\{\mathbf{y}^1, \dots, \mathbf{y}^T\}$
 - 2: **for** $c = 1, \dots, C$ **do**
 - 3: **for** $t = 2, \dots, T$ **do**
 - 4: Generate s MCMC samples $\mathbf{y}_1^t, \dots, \mathbf{y}_s^t$ from $P(\mathbf{y}^t | \mathbf{y}^{t-1}; \eta_{c-1})$
 - 5: Calculate $\boldsymbol{\mu}_t = s^{-1} \sum_{i'=1}^s \mathbf{g}(\mathbf{y}_{i'}^t | \mathbf{y}^{t-1})$
 - 6: Calculate $\boldsymbol{\Sigma}_t = s^{-1} \sum_{i'=1}^s \mathbf{g}(\mathbf{y}_{i'}^t | \mathbf{y}^{t-1}) \mathbf{g}(\mathbf{y}_{i'}^t | \mathbf{y}^{t-1})^\top - \boldsymbol{\mu}_t \boldsymbol{\mu}_t^\top$
 - 7: **end for**
 - 8: Calculate $\hat{\mathbf{S}}(\eta_{c-1}) = \sum_{t=2}^T [\mathbf{g}(\mathbf{y}^t | \mathbf{y}^{t-1}) - \boldsymbol{\mu}_t]$ and $\hat{\mathbf{H}}(\eta_{c-1}) = - \sum_{t=2}^T \boldsymbol{\Sigma}_t$
 - 9: $\eta_c = \eta_{c-1} - \hat{\mathbf{H}}(\eta_{c-1})^{-1} \hat{\mathbf{S}}(\eta_{c-1})$
 - 10: **end for**
 - 11: $\tilde{\eta} \leftarrow \eta_c$
 - 12: **Output:** learned parameter $\tilde{\eta}$
-

In this work, for parameter learning, each sampled network using CD_K sampling is generated after K transitions starting from the observed network \mathbf{y}^t , so a burn-in phase is not required and a tremendous sample size is not indispensable. A small value of K can be used in practice, especially for fast initialization of [Algorithm 1](#) and good refinement of [Algorithm 2](#): the CD_K sampling is in favor of the normality approximation from [Hummel et al. \(2012\)](#) since each sampled $\mathbf{y}_{i'}^t$ is only K dyads different from the observed \mathbf{y}^t , and the network statistics of the MCMC samples are close to those of the observed networks when the learned parameter is close to the MLE.

However, a small value of K in [Algorithm 1](#) generates a pseudo-observation of [Equation \(6\)](#) that is not distinct from $\sum_{t=2}^T \mathbf{g}(\mathbf{y}^t | \mathbf{y}^{t-1})$, which may compromise the advantage of the partial stepping from [Hummel et al. \(2012\)](#). Hence, a trade-off among the number of transitions K , sample size s , and learning iteration C is needed for the purpose of implementation. See [Krivitsky \(2017\)](#) for a detailed study of using Contrastive Divergence in ERGM fitting, especially regarding the choice of hyperparameters and stopping criterion. The CD_K sampling algorithm to generate a single sampled network $\mathbf{y}_{i'}^t$ is provided in [Algorithm 3](#), and it is used in [Step 4](#) of [Algorithm 1](#) and [Step 4](#) of [Algorithm 2](#).

The complexity of [Algorithm 3](#) to sample one valued network with K MCMC transitions is $O(K\mathcal{C}_\alpha)$. The term \mathcal{C}_α is the complexity of calculating the acceptance ratio α with [Equation \(8\)](#), which depends on the user's choice of the network statistics for both augmentation and diminution

Algorithm 3 Contrastive Divergence sampling

- 1: **Input:** MCMC transition step K , parameter $\boldsymbol{\eta} = (\boldsymbol{\eta}^+, \boldsymbol{\eta}^-)$, $\{\mathbf{y}^{t-1}, \mathbf{y}^t\}$
 - 2: Set $\tilde{\mathbf{y}} = \mathbf{y}^t$
 - 3: **for** $k = 1, \dots, K$ **do**
 - 4: Choose randomly a dyad (i, j) s.t. $i \neq j$
 - 5: Propose a dyad value $\tilde{\mathbf{y}}_{ij}^{k+1}$ from Equation (7)
 - 6: Calculate the acceptance ratio α for $\tilde{\mathbf{y}}_{ij}^{k+1}$ from Equation (8)
 - 7: **if** $\text{uniform}(0, 1) < \alpha$ **then**
 - 8: Accept $\tilde{\mathbf{y}}_{ij}^{k+1}$
 - 9: **end if**
 - 10: **end for**
 - 11: **Output:** a sampled network $\tilde{\mathbf{y}}$
-

processes as well as the randomness of the proposed dyad values from Equation (7). Likewise, for Algorithm 1, the complexity to sample s valued networks in Step 4 is $O(sKC_\alpha)$. In Steps 5 and 6 of Algorithm 1, the complexity of calculating the mean vector $\boldsymbol{\mu}_t \in \mathbb{R}^p$ and the covariance matrix $\boldsymbol{\Sigma}_t \in \mathbb{R}^{p \times p}$ of s sampled network statistics is $O(s\mathcal{C}_{2g} + sp + sp^2)$. The term \mathcal{C}_{2g} is the complexity to calculate the two network statistics $\mathbf{g}(\mathbf{y}^t | \mathbf{y}^{t-1}) = [\mathbf{g}^+(\mathbf{y}^{+,t} | \mathbf{y}^{t-1}), \mathbf{g}^-(\mathbf{y}^{-,t} | \mathbf{y}^{t-1})] \in \mathbb{R}^p$ that are based on the user's choice. Finally, the complexity of calculating the pseudo-observation $\hat{\boldsymbol{\xi}}(\mathbf{y})$ and the maximizer $\tilde{\boldsymbol{\eta}}$ in Steps 8 and 9 of Algorithm 1 is $O(T\mathcal{C}_{2g} + T + p^2)$, where T is the number of observed networks. Overall, the complexity of Algorithm 1 is $O(C[T(sKC_\alpha + s\mathcal{C}_{2g} + sp + sp^2) + T\mathcal{C}_{2g} + T + p^2])$, where C is the number of learning iterations. The complexity of Algorithm 2 is similar, except for different choices of the input parameters and MCMC variation in the proposed dyad values.

5 Experiments

In this section, we apply PST ERGM on two simulated data and two real data. The network statistics of interest are chosen from a comprehensive list in Handcock et al. (2021), and the choices for the augmentation process are identical to those for the diminution process. For real data experiments, the details and formulations of selected network statistics are provided in the Appendix.

5.1 Simulation Study 1

In this experiment with $T = 2$, we test our Metropolis-Hastings algorithm by generating \mathbf{y}^2 with pre-defined parameters $\boldsymbol{\eta}^+$ and $\boldsymbol{\eta}^-$ conditional on a fixed valued network \mathbf{y}^1 . We then test our parameter learning algorithms by estimating the coefficients from sampled networks to compare with the true parameters. We choose the following three network statistics displayed in Table 2 for both augmentation and diminution processes.

For the artificial data, we use Algorithm 3 to generate 100 sampled networks $\mathbf{y}^2 \in \mathbb{N}_0^{n \times n}$ conditioning on the initialized $\mathbf{y}^1 \in \mathbb{N}_0^{n \times n}$, with parameter $\boldsymbol{\eta}^+ = (-2, 1, 1)$, $\boldsymbol{\eta}^- = (-1, 1, 1)$, the number of nodes $n = 50$, and the maximum dyad value of diminution networks $m = 3$. To ensure the simulated networks are sampled in a general setting with reasonable mixing, we initialize each

Network Statistics	$\mathbf{g}(\mathbf{y})$
Edge sum	$\sum_{ij} \mathbf{y}_{ij}$
Mutuality	$\sum_{i < j} \sqrt{\mathbf{y}_{ij} \mathbf{y}_{ji}}$
Transitive weight	$\sum_{ij} \min(\mathbf{y}_{ij}, \max_{k \in N} (\min(\mathbf{y}_{ik}, \mathbf{y}_{kj})))$

Table 2: Network statistics for simulation study.

sampling chain of a network from an uninformative starting point and run it for a relatively long period. Specifically, each sampled network \mathbf{y}^2 is generated after $K = 10 \times n \times n$ MCMC transitions of Algorithm 3, starting from an all-ones matrix with zeros on the diagonal.

In comparison with the true parameters, we learn the approximate MLE $\tilde{\boldsymbol{\eta}} = (\tilde{\boldsymbol{\eta}}^+, \tilde{\boldsymbol{\eta}}^-)$ of our proposed PST ERGM $P(\mathbf{y}^2 | \mathbf{y}^1)$, for each of the 100 simulated networks \mathbf{y}^2 . To avoid the reliance on starting points in parameter estimation, we initialize $\boldsymbol{\eta}_0$ of Algorithm 1 as zero vector throughout this experiment. Subsequently, for fast initialization and refinement of the estimated parameters, we let the sampling chain, which starts from the input network \mathbf{y}^2 , to be relatively short during the learning process. In particular, we implement $C = 20$ iterations of Algorithm 1, followed by $C = 5$ iterations of Algorithm 2. An MCMC sample size of $s = 100$ and $s = 1000$ for CD_n sampling of Algorithm 3 is used in Algorithm 1 and 2 respectively, where $K = n = 50$ is the number of MCMC transitions.

The absolute values of median and standard deviation of $\tilde{\boldsymbol{\eta}}^+ - \boldsymbol{\eta}^+$ over 100 simulations are reported in Table 3. The corresponding results for $\tilde{\boldsymbol{\eta}}^- - \boldsymbol{\eta}^-$ are reported in Table 4. On average, the estimations are close to the true parameters as the absolute values of median of the differences are close to 0.

# of time step & node	$ \tilde{\boldsymbol{\eta}}_1^+ - \boldsymbol{\eta}_1^+ $	$ \tilde{\boldsymbol{\eta}}_2^+ - \boldsymbol{\eta}_2^+ $	$ \tilde{\boldsymbol{\eta}}_3^+ - \boldsymbol{\eta}_3^+ $
$T = 2, n = 50$	0.098 (0.181)	0.055 (0.171)	0.015 (0.172)

Table 3: Absolute values of median (standard deviation) of $\tilde{\boldsymbol{\eta}}^+ - \boldsymbol{\eta}^+$ over 100 simulations.

# of time step & node	$ \tilde{\boldsymbol{\eta}}_1^- - \boldsymbol{\eta}_1^- $	$ \tilde{\boldsymbol{\eta}}_2^- - \boldsymbol{\eta}_2^- $	$ \tilde{\boldsymbol{\eta}}_3^- - \boldsymbol{\eta}_3^- $
$T = 2, n = 50$	0.003 (0.235)	0.024 (0.149)	0.114 (0.193)

Table 4: Absolute values of median (standard deviation) of $\tilde{\boldsymbol{\eta}}^- - \boldsymbol{\eta}^-$ over 100 simulations.

5.2 Simulation Study 2

In this experiment, we simulate a sequence of dynamic valued networks $\mathbf{y}^1, \dots, \mathbf{y}^T \in \mathbb{N}_0^{n \times n}$ with pre-defined parameters, and we estimate the coefficients from sampled networks to compare with the true parameters. We let the time step $T = 5, 10, 15$ and the number of nodes $n = 50, 100$. The three network statistics from Simulation Study 1 are used here.

To simulate the artificial networks, we initialize $\boldsymbol{\eta}^+ = (-2, 1, 1)$, $\boldsymbol{\eta}^- = (-1, 1, 1)$, the maximum dyad value of diminution networks $m = 3$, and a fixed valued network $\mathbf{y}^1 \in \mathbb{N}_0^{n \times n}$ for $n = 50$ and $n = 100$ respectively. For $t = 2, \dots, T$, we use Algorithm 3 to sample \mathbf{y}^t , conditioning on

the previously sampled network \mathbf{y}^{t-1} . To ensure the networks are sampled with reasonable mixing that does not depend on initialization, each sampled \mathbf{y}^t is generated after $K = 20 \times n \times n$ MCMC transitions of Algorithm 3, starting from an all-ones matrix with zeros on the diagonal. We repeat the process until we have $\mathbf{y}^1, \dots, \mathbf{y}^T$ for each combination of T and n .

To compare with the true parameters, we learn the approximate MLE $\tilde{\boldsymbol{\eta}} = (\tilde{\boldsymbol{\eta}}^+, \tilde{\boldsymbol{\eta}}^-)$ of our proposed PST ERGM $\prod_{t=2}^T P(\mathbf{y}^t | \mathbf{y}^{t-1})$ for the simulated networks $\mathbf{y}^1, \dots, \mathbf{y}^T$. To efficiently seed an initial configuration, we first apply $C = 20$ iterations of Algorithm 1 with zero vectors as initialized $\boldsymbol{\eta}_0$. An MCMC sample size of $s = 100$ with CD_n sampling is applied for each time t , where the MCMC transitions K is set to the corresponding network size n . Subsequently, to refine the parameters, we apply $C = 5$ iterations of Algorithm 2, where an MCMC sample size of $s = 1000$ with CD_n sampling is used for each time t . We estimate the coefficients of $\prod_{t=2}^T P(\mathbf{y}^t | \mathbf{y}^{t-1})$ repeatedly for 100 times. The absolute values of median and standard deviation of $\tilde{\boldsymbol{\eta}}^+ - \boldsymbol{\eta}^+$ over 100 estimations for each combination of T and n are reported in Table 5. The corresponding results for $\tilde{\boldsymbol{\eta}}^- - \boldsymbol{\eta}^-$ are reported in Table 6.

We notice in the results that the estimated parameters are close to the true parameters, as the absolute values of median of the differences are close to 0. For a fixed network size n in either augmentation or diminution process, the standard deviations of the estimated parameters decrease as the number of time step T increases, which is expected as we have more temporal data for the estimation.

# of time step & node	$ \tilde{\boldsymbol{\eta}}_1^+ - \boldsymbol{\eta}_1^+ $	$ \tilde{\boldsymbol{\eta}}_2^+ - \boldsymbol{\eta}_2^+ $	$ \tilde{\boldsymbol{\eta}}_3^+ - \boldsymbol{\eta}_3^+ $
$T = 5, n = 50$	0.016 (0.019)	0.069 (0.012)	0.061 (0.016)
$T = 5, n = 100$	0.036 (0.019)	0.125 (0.016)	0.030 (0.014)
$T = 10, n = 50$	0.106 (0.011)	0.059 (0.010)	0.127 (0.009)
$T = 10, n = 100$	0.017 (0.011)	0.006 (0.011)	0.013 (0.008)
$T = 15, n = 50$	0.023 (0.010)	0.019 (0.010)	0.002 (0.007)
$T = 15, n = 100$	0.006 (0.009)	0.013 (0.008)	0.012 (0.006)

Table 5: Absolute values of median (standard deviation) of $\tilde{\boldsymbol{\eta}}^+ - \boldsymbol{\eta}^+$ over 100 estimations.

# of time step & node	$ \tilde{\boldsymbol{\eta}}_1^- - \boldsymbol{\eta}_1^- $	$ \tilde{\boldsymbol{\eta}}_2^- - \boldsymbol{\eta}_2^- $	$ \tilde{\boldsymbol{\eta}}_3^- - \boldsymbol{\eta}_3^- $
$T = 5, n = 50$	0.034 (0.028)	0.119 (0.021)	0.053 (0.023)
$T = 5, n = 100$	0.080 (0.026)	0.012 (0.015)	0.080 (0.026)
$T = 10, n = 50$	0.069 (0.018)	0.101 (0.015)	0.007 (0.017)
$T = 10, n = 100$	0.028 (0.019)	0.041 (0.010)	0.014 (0.019)
$T = 15, n = 50$	0.057 (0.015)	0.053 (0.011)	0.064 (0.014)
$T = 15, n = 100$	0.032 (0.015)	0.024 (0.008)	0.066 (0.015)

Table 6: Absolute values of median (standard deviation) of $\tilde{\boldsymbol{\eta}}^- - \boldsymbol{\eta}^-$ over 100 estimations.

5.3 Modeling: Students Contact Data

[Mastrandrea et al. \(2015\)](#) used wearable sensors to detect face-to-face contacts between students among nine classes in a high school. The real-time contact events are logged for every 20-second

interval of any two students within a physical distance of 1.5 meters, from 02-Dec-2013 to 06-Dec-2013. Additionally, online social network (Facebook) was submitted by the students voluntarily. In this demonstration, we model student interactions within one of the nine classes, whose class name is MP. There are $n = 29$ students which consist of 11 females and 18 males. Four students with no recorded gender are excluded. We divide the entries by day to construct $T = 5$ undirected valued networks, where \mathbf{y}_{ij}^t is the number of unique contacts between student i and student j in day t regardless of the duration of each contact. Also, nodal covariate $\mathbf{x}_i \in \{\text{F}, \text{M}\}$ is the gender of student i , and dyadic covariate $e_{ij} \in \{1, 0\}$ indicates whether student i and student j are friends on Facebook or not. The valued networks across five days and the binary network for Facebook friendship are visualized in Figure 3. The color and shape of nodes represent the gender of students. The darkness and thickness of edges show the number of unique contacts.

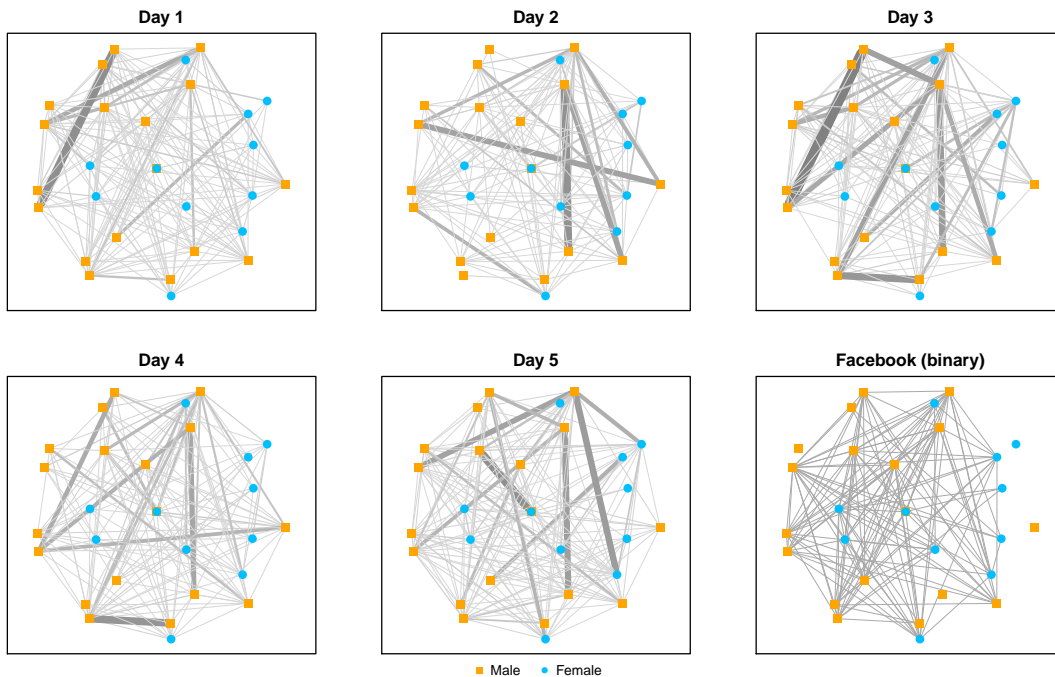


Figure 3: Students contact data of class MP across five days and Facebook network.

We choose six network statistics of interest for analysis, and we learn a time-heterogeneous PST ERGM $\prod_{t=2}^5 P(\mathbf{y}^t | \mathbf{y}^{t-1}; \boldsymbol{\eta}^t)$ for the data. A time-homogeneous model was attempted, but the large variation between different intervals suggests that a time-heterogeneous model is appropriate and realistic. The estimated coefficients and standard errors for the augmentation process are reported in Table 7. The corresponding results for the diminution process are reported in Table 8. The standard errors are obtained from the Fisher Information matrix $\mathbf{I}(\boldsymbol{\eta}^t) \approx -\hat{\mathbf{H}}(\tilde{\boldsymbol{\eta}}^t)$ of Equation (5) evaluated at the learned parameter.

The positive coefficients on the edge sum term in the augmentation process from $t = 2$ to $t = 5$ indicate frequent interactions among students throughout the week. However, the negative coefficients on the edge sum term in the diminution process from $t = 3$ to $t = 5$ suggest a short duration on the continuing increment of contact occurrences. In other words, the number of contacts between students fluctuates over time, which also supports the adoption of a time-heterogeneous model. Similarly, the highly negative coefficients on the dispersion term in both

Network Statistics	$\eta^{+,2}$	$\eta^{+,3}$	$\eta^{+,4}$	$\eta^{+,5}$
Edge sum	3.218 (0.093)	3.337 (0.091)	3.021 (0.107)	3.195 (0.081)
Dispersion	-6.824 (0.222)	-7.569 (0.192)	-6.467 (0.227)	-6.503 (0.200)
Homophily (M)	0.148 (0.074)	0.201 (0.075)	0.100 (0.084)	0.137 (0.061)
Heterophily (M-F)	0.040 (0.072)	0.058 (0.076)	0.072 (0.080)	0.057 (0.059)
Facebook	-0.005 (0.043)	0.126 (0.030)	-0.034 (0.047)	0.092 (0.035)
Transitive weight	-0.143 (0.035)	-0.068 (0.025)	-0.018 (0.046)	-0.188 (0.031)

Coefficients statistically significant at 0.05 level are bolded.

Table 7: Parameter estimation (standard error) of $\eta^{+,t}$ for the students contact data.

Network Statistics	$\eta^{-,2}$	$\eta^{-,3}$	$\eta^{-,4}$	$\eta^{-,5}$
Edge sum	0.424 (0.217)	-0.980 (0.213)	-0.636 (0.188)	-0.294 (0.168)
Dispersion	-6.558 (0.281)	-6.161 (0.330)	-6.083 (0.278)	-6.678 (0.274)
Homophily (M)	-0.157 (0.181)	1.340 (0.208)	0.671 (0.185)	0.389 (0.148)
Heterophily (M-F)	-0.215 (0.185)	0.483 (0.167)	-0.208 (0.189)	0.103 (0.154)
Facebook	-0.083 (0.090)	0.227 (0.101)	0.193 (0.086)	0.097 (0.080)
Transitive weight	0.084 (0.065)	-0.435 (0.074)	-0.444 (0.043)	-0.075 (0.046)

Coefficients statistically significant at 0.05 level are bolded.

Table 8: Parameter estimation (standard error) of $\eta^{-,t}$ for the students contact data.

augmentation and diminution processes suggest a strong degree of overdispersion in the number of contacts. This can be verified by the high standard deviation of non-zero dyad values across five days, which is 10.2, whereas the mean is about half in magnitude, which is 5.8.

In the augmentation process from $t = 2$ to $t = 5$, the positive coefficients on the homophily for males suggest a strong effect of gender in promoting more interactions among male students. Additionally, their positive coefficients in the diminution process from $t = 3$ to $t = 5$ indicate that the active interactions among male students tend to be ongoing once they have begun. However, these effects are less significant for students of different genders, given the imbalanced proportion between females and males. As supporting evidence, about 89% or 136 out of $\binom{18}{2} = 153$ pairs of male students have contact events logged by sensors, and their average span is $\frac{1}{136} \sum_{t=1}^5 \sum_{i<j} \mathbf{I}(\mathbf{y}_{ij}^t > 0 \wedge \mathbf{x}_i = \mathbf{M} \wedge \mathbf{x}_j = \mathbf{M}) \approx 2.8$ days. In contrast, about 71% or 141 out of 198 pairs of male and female students have contact events logged, and their average span is $\frac{1}{141} \sum_{t=1}^5 \sum_{i<j} \mathbf{I}(\mathbf{y}_{ij}^t > 0 \wedge \mathbf{x}_i \neq \mathbf{x}_j) \approx 2.3$ days.

Furthermore, in the augmentation process from $t = 2$ to $t = 5$, the alternating signs of coefficients on the Facebook term indicate that if two students are friends online, they occasionally have active interactions in school. However, the majority of positive coefficients on the Facebook term in the diminution process suggest that online friendships maintain offline interactions as time passes. About 82% or 119 out of 145 reported Facebook friendships have contact events logged in school, and their average span is $\frac{1}{119} \sum_{t=1}^5 \sum_{i<j} \mathbf{I}(\mathbf{y}_{ij}^t > 0 \wedge e_{ij} = 1) \approx 2.9$ days. Lastly, the transitive relationship in the number of contacts is weak, as indicated by the negative coefficients on the transitivity weights in the augmentation process. The majority of negative coefficients in the diminution process suggest that the transitivity tends not to persist over time. These outcomes can

be observed visually from Figure 3, where most triads are closed with thin edges, and the triangular patterns fluctuate throughout the week.

To validate the learned model heuristically, we simulate networks with the estimated parameters from Tables 7 and 8 to compare the sampled network statistics with the observed network statistics. For $t = 2, \dots, 5$, we generate 100 valued networks \mathbf{y}^t conditional on the observed \mathbf{y}^{t-1} , where each sampled network is generated after $K = 200 \times n \times n$ MCMC transitions starting from an all-ones matrix with zeros on the diagonal. Once they are obtained, we construct the corresponding $\mathbf{y}^{+,t}$ and $\mathbf{y}^{-,t}$ and calculate their network statistics. The distribution of the simulated network statistics and the observed network statistics values in red lines are displayed in Figure 4. Overall, the simulated network statistics align with the observed network statistics, suggesting that the learned time-heterogeneous PST ERGM $\prod_{t=2}^5 P(\mathbf{y}^t | \mathbf{y}^{t-1}; \boldsymbol{\eta}^t)$ is a good representation of the observed data in terms of the six selected network statistics.

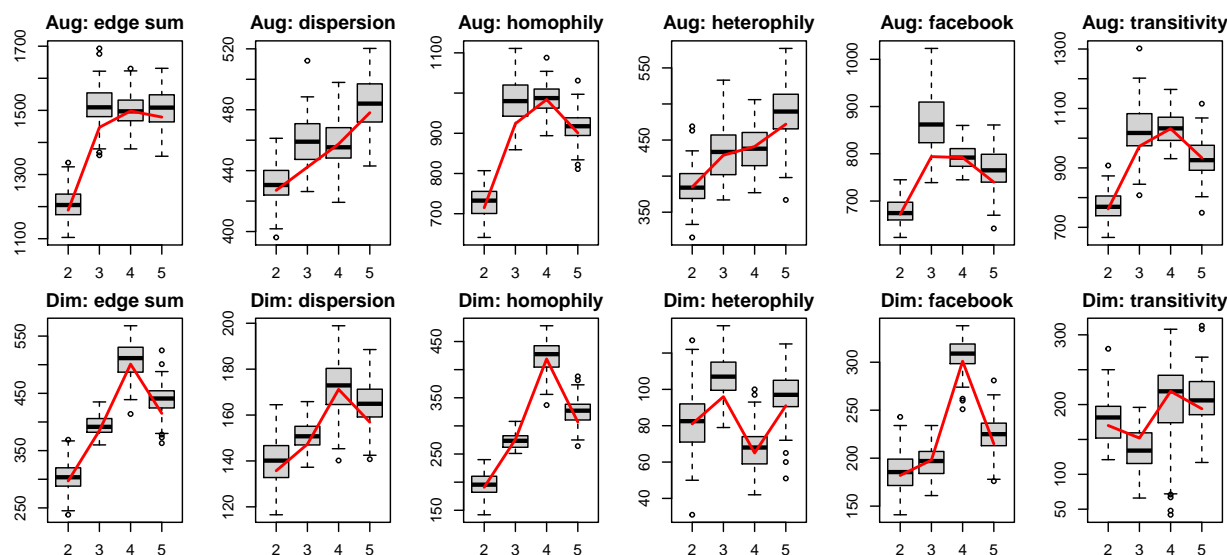


Figure 4: The distribution of the sampled network statistics (box plots) and the observed network statistics values (red lines) across four consecutive intervals for augmentation (Aug) and diminution (Dim) process.

5.4 Forecasting: Baboons Interaction Data

Gelardi et al. (2020) studied the interactions among $n = 13$ Guinea baboons for a duration of 28 days. With sensors attached to their collars, contact events are recorded for every 20-second interval of any two primates within proximity of 1.5 meters. The data is divided by day to construct a sequence of $T = 28$ undirected valued networks, where \mathbf{y}_{ij}^t is the number of unique contacts between baboon i and baboon j in day t regardless of the duration of each contact. In this experiment, we focus on forecasting future temporal trends with the model learned from the past data. Specifically, we learn a time-homogeneous PST ERGM based on the data from day 1 to day 23, and then we forecast networks for the 5 subsequent time points to compare with the observed networks from day 24 to day 28. Though a time-heterogeneous model can learn the transitions between consecutive time points well, it lacks the ability to forecast future networks as a learned

parameter η^t is tailored to the designated time point t and cannot be extended to the next time point $t + 1$.

We choose four network statistics for this task. The estimated parameters and standard errors for both augmentation and diminution processes are reported in Table 9. To forecast out-of-sample data, we generate 100 valued network \hat{y}^t conditional on the observed network y^{t-1} for $t = 24, \dots, 28$. To avoid dependence on the initialization, each sampled network is generated after $K = 200 \times n \times n$ MCMC transitions starting from an all-ones matrix with zeros on the diagonal. Once the forecasted networks are obtained, we construct the corresponding $\hat{y}^{+,t}$ and $\hat{y}^{-,t}$ and calculate their network statistics. The distribution of the forecasted network statistics and the observed network statistics values in red lines are displayed in Figure 5.

Network Statistics	η^+	η^-
Edge sum	4.673 (0.017)	-0.159 (0.014)
Propensity	9.933 (0.205)	10.349 (0.157)
Dispersion	-14.718 (0.139)	-14.065 (0.104)
Transitive weight	-0.060 (0.014)	-0.146 (0.007)

Coefficients statistically significant at 0.05 level are bolded.

Table 9: Parameter estimation (standard error) for the baboons data from day 1 to 23.

In exchange for the extrapolation of future temporal trends, the time-homogeneous PST ERGM that consolidates the fluctuation of structural property throughout 23 days into one parameter η may introduce variation to the forecasted network statistics. The discrepancy on day 25 is potentially impacted by this outcome. Furthermore, the discrepancy of the propensity term on day 27 in the diminution process may be influenced by the increment of all network statistics from day 26 in both augmentation and diminution processes, as our proposed PST ERGM allows interaction between the two processes. Note that in PST ERGM, the augmentation network and diminution network are no longer conditionally independent as the sample space of valued networks becomes infinite. In summary, besides prediction error for the unseen data, the learned time-homogeneous PST ERGM effectively recovers the sudden change on day 26 along with the temporal trends from day 24 to 28.

Another aspect worth mentioning is the comparison between the edge sum term and the propensity term in this experiment. The propensity term $\sum_{i < j} \mathbf{I}(y_{ij} > 0)$ serves as a thresholding network statistics of the edge sum term $\sum_{i < j} y_{ij}$. Although the observed edge sums along with the other two network statistics, dispersion and transitivity, in red lines of Figure 5 show a decreasing trend followed by an increasing trend from day 24 to 28, the observed propensities primarily show a decreasing trend in both augmentation and diminution processes. In alignment with the motivation of valued ERGM (Krivitsky, 2012), dichotomizing valued networks into binary networks or dyad value thresholding for network analysis may introduce biases (Thomas and Blitzstein, 2011) that result in unrealistic interpretation of the network dynamics. As opposed to modeling the snapshots of observed networks, the parsimonious PST ERGM not only dissects the intermediary dynamics of evolving valued networks, but also provides the ability to forecast future trends reasonably.

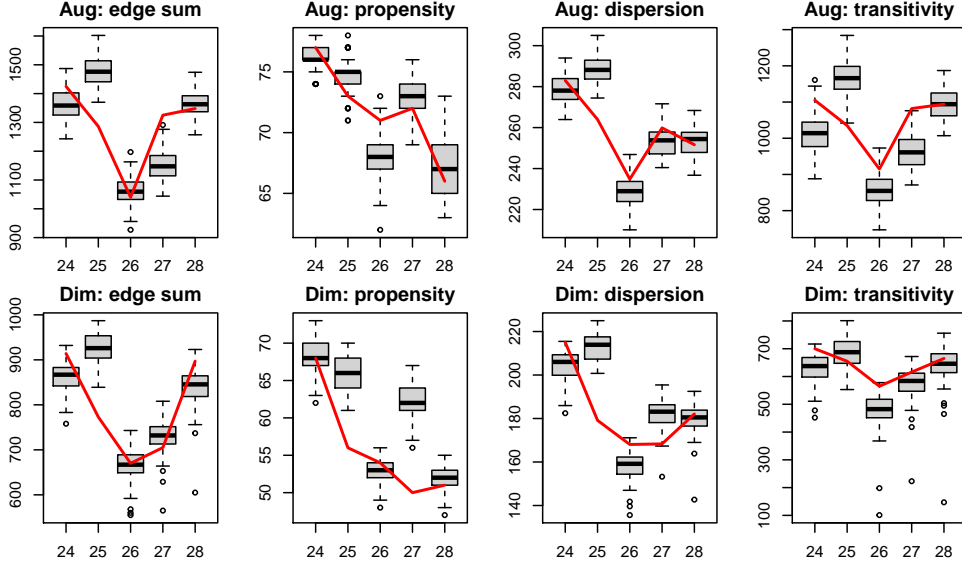


Figure 5: The distribution of the forecasted network statistics (box plots) and the observed network statistics values (red lines) for augmentation (Aug) and diminution (Dim) process from day 24 to day 28.

6 Discussion

This paper introduces a probability distribution of dynamic valued networks. In reality, the factors and processes that increase relational strength are usually different from those that decrease relational strength. While dynamic network models should capture the intrinsic difference between consecutive networks, models neglecting the confounding effect of structural change may result in misinterpretation of network evolution. In this article, we generalize the STERGM from Krivitsky and Handcock (2014) to dissect the network transition with two intermediate networks, where one collects dyad value augmentation, and the other collects dyad value diminution. Our proposed PST ERGM provides the interpretability of network evolution and the capability to forecast temporal trends. Our algorithms inherit the state-of-the-art estimation techniques of ERGM frameworks.

The MCMC-based Maximum Likelihood Estimation algorithms remain computational intensive and require careful initialization. To align with the model’s assumption and to address the challenge that the model is no longer fully separable, we estimate the parameters by drawing MCMC samples from the space of \mathbf{y}^t with acceptance based on the construction of the augmentation network $\mathbf{y}^{+,t}$ and the diminution network $\mathbf{y}^{-,t}$. With Contrastive Divergence sampling to speed up parameter estimation, we seed an adequate initialized configuration with partial stepping on the log-likelihood ratio and we refine the parameter near its convergence by directly maximizing the log-likelihood. However, this mutually beneficial combination requests further deliberation to balance the accuracy of estimation and the burden of computation.

Several improvements to the PST ERGM framework are possible for future development. We can extend the sample space \mathcal{Y}^t to networks with continuous dyad values $\mathbf{y}_{ij}^t \in \mathbb{R}$, since it will include more real-world situations where precise relational strength is recorded. In this setting, a proper redefinition of the reference functions $h(\mathbf{y}^t|\mathbf{y}^{t-1})$ and network statistics $\mathbf{g}(\mathbf{y}^t|\mathbf{y}^{t-1})$ is needed as PST ERGM becomes a continuous probability distribution. Furthermore, besides

dyad value augmentation where $\mathbf{y}_{ij}^{+,t} = \max(\mathbf{y}_{ij}^{t-1}, \mathbf{y}_{ij}^t)$ and dyad value diminution where $\mathbf{y}_{ij}^{-,t} = \min(\mathbf{y}_{ij}^{t-1}, \mathbf{y}_{ij}^t)$, we can allow alternative ways to dissect network evolution, as long as the confounding effects of network dynamic is avoided. Over time, the number of participants in a system and the process that induces their relation may not be fixed or completely observed. It is of great importance for a dynamic network model to identify the temporal changes punctually (e.g., Padilla et al., 2019; Yu et al., 2021) and to adjust the structural changes accordingly as discussed in Krivitsky et al. (2011). Finally, model degeneracy that is studied theoretically in Handcock et al. (2003) is a well-known challenge in ERGM framework. Therefore, a rigorous way to design more informative network statistics as in Snijders et al. (2006) and a systematic way to evaluate the goodness of model fit as in Hunter et al. (2008a) are needed for dynamic valued networks. The tapered ERGM introduced in Fellows and Handcock (2017), and Blackburn and Handcock (2022) can also be extended to the PST ERGM to alleviate the degeneracy problem.

Acknowledgement

Code to implement our methodology can be found at <https://github.com/allenkei/PSTERGM>. The real data analyzed in Section 5.3 is publicly available at <http://www.sociopatterns.org/datasets/high-school-contact-and-friendship-networks/>. The real data analyzed in Section 5.4 is publicly available at <https://osf.io/ufs3y/>. We thank Mark Handcock for helpful comments on this work.

This research did not receive any specific grant from funding agencies in the public, commercial, or not-for-profit sectors. All authors declare that they have no conflicts of interest.

A Experiment Details

In this section, we provide the formulations of selected network statistics used in the two real data examples. The network statistics of interest are chosen from a comprehensive list in [Handcock et al. \(2021\)](#), an R library for social network analysis. The choices of network statistics for the augmentation process are identical to those for the diminution process. Furthermore, we provide the learning schedules of the two experiments.

A.1 Students Contact Data

The formulations of six network statistics used for the students contact data ([Mastrandrea et al., 2015](#)) are displayed in Table 10. In this time-heterogeneous PST ERGM $\prod_{t=2}^5 P(\mathbf{y}^t | \mathbf{y}^{t-1}; \boldsymbol{\eta}^t)$, the parameter $\boldsymbol{\eta}^t$ is learned sequentially for $t = 2, \dots, 5$, and we initialize $\boldsymbol{\eta}_0^t$ of Algorithm 1 as zero vector.

Network Statistics	$\mathbf{g}(\mathbf{y})$
Edge sum	$\sum_{i < j} \mathbf{y}_{ij}$
Dispersion	$\sum_{i < j} \sqrt{\mathbf{y}_{ij}}$
Homophily (M)	$\sum_{i < j} \mathbf{y}_{ij} \times \mathbf{I}(\mathbf{x}_i = \mathbf{M} \wedge \mathbf{x}_j = \mathbf{M})$
Heterophily (M-F)	$\sum_{i < j} \mathbf{y}_{ij} \times \mathbf{I}(\mathbf{x}_i \neq \mathbf{x}_j)$
Facebook	$\sum_{i < j} \mathbf{y}_{ij} \times \mathbf{e}_{ij}$
Transitive weight	$\sum_{i < j} \min(\mathbf{y}_{ij}, \max_{k \in N} (\min(\mathbf{y}_{ik}, \mathbf{y}_{kj})))$

Table 10: Network statistics for the students contact data.

To seed an initial configuration for each $\boldsymbol{\eta}^t$, we implement $C = 20$ iterations of Algorithm 1 where an MCMC sample size of $s = 100$ with $\text{CD}_{5 \times n}$ sampling is used, followed by another $C = 20$ iterations of Algorithm 2 where an MCMC sample size of $s = 100$ with $\text{CD}_{10 \times n}$ sampling is used. The term n is the number of students in this data, which is 29. Subsequently, to refine the learned parameters, we implement $C = 10$ iterations of Algorithm 2 where an MCMC sample size of $s = 1000$ with $\text{CD}_{25 \times n \times n}$ sampling is used.

Finally, the standard errors are obtained from the Fisher Information matrix $\mathbf{I}(\boldsymbol{\eta}^t) \approx -\hat{\mathbf{H}}(\tilde{\boldsymbol{\eta}}^t)$ of Equation (5) evaluated at the learned parameter $\tilde{\boldsymbol{\eta}}^t$ with 1000 sampled networks. Each sampled network is generated after $K = 20 \times n \times n$ MCMC transitions starting from observed \mathbf{y}^t .

A.2 Baboons Interaction Data

The formulations of four network statistics used for the baboons interaction data ([Gelardi et al., 2020](#)) are displayed in Table 11. In this time-homogeneous PST ERGM $\prod_{t=2}^{23} P(\mathbf{y}^t | \mathbf{y}^{t-1})$, the parameter $\boldsymbol{\eta}$ is shared across $t = 2, \dots, 23$ and is also used to forecast the temporal trends for $t = 24, \dots, 28$. We initialize $\boldsymbol{\eta}_0$ of Algorithm 1 as zero vector.

To seed an initial configuration for $\boldsymbol{\eta}$, we implement $C = 20$ iterations of Algorithm 1 where an MCMC sample size of $s = 100$ with CD_n sampling is used for each time t , followed by another $C = 20$ iterations of Algorithm 2 where an MCMC sample size of $s = 100$ with $\text{CD}_{2 \times n}$ sampling is used for each time t . The term n is the number of baboons in this data, which is 13. Subsequently,

Network Statistics	$g(\mathbf{y})$
Edge sum	$\sum_{i<j} \mathbf{y}_{ij}$
Propensity	$\sum_{i<j} \mathbf{I}(\mathbf{y}_{ij} > 0)$
Dispersion	$\sum_{i<j} \sqrt{\mathbf{y}_{ij}}$
Transitive weight	$\sum_{i<j} \min(\mathbf{y}_{ij}, \max_{k \in N} (\min(\mathbf{y}_{ik}, \mathbf{y}_{kj})))$

Table 11: Network statistics for the baboons interaction data.

to refine the learned parameter, we implement $C = 10$ iterations of Algorithm 2 where an MCMC sample size of $s = 1000$ with $\text{CD}_{50 \times n \times n}$ sampling is used for each time t . In this experiment, we also let the maximum dyad value of diminution networks $m = 200$, a moderate upper bound that is greater than the highest dyad value of diminution networks $\mathbf{y}^{-,2}, \dots, \mathbf{y}^{-,28}$ constructed from the observed networks.

Finally, the standard errors are obtained from the Fisher Information matrix $\mathbf{I}(\boldsymbol{\eta}) \approx -\hat{\mathbf{H}}(\tilde{\boldsymbol{\eta}})$ of Equation (5) evaluated at the learned parameter $\tilde{\boldsymbol{\eta}}$ with 1000 sampled networks for each time t . Each sampled network is generated after $K = 20 \times n \times n$ MCMC transitions starting from observed \mathbf{y}^t .

References

- Bart Blackburn and Mark S Handcock. Practical network modeling via tapered exponential-family random graph models. Journal of Computational and Graphical Statistics, pages 1–14, 2022.
- Tom Broekel and Marcel Bednarz. Disentangling link formation and dissolution in spatial networks: An application of a two-mode stergm to a project-based r&d network in the german biotechnology industry. Networks and Spatial Economics, 18(3):677–704, 2018.
- Alberto Caimo and Isabella Gollini. A multilayer exponential random graph modelling approach for weighted networks. Computational Statistics & Data Analysis, 142:106825, 2020.
- Miguel A Carreira-Perpinan and Geoffrey Hinton. On contrastive divergence learning. In International workshop on Artificial Intelligence and Statistics, pages 33–40. PMLR, 2005.
- Skyler J Cranmer and Bruce A Desmarais. Inferential network analysis with exponential random graph models. Political analysis, 19(1):66–86, 2011.
- Jiaying Deng, Mingwen Yang, M. Pelster, and Yong Tan. A boon or a bane? an examination of social communication in social trading. Capital Markets: Market Efficiency eJournal, 2021.
- Bruce A Desmarais and Skyler J Cranmer. Statistical inference for valued-edge networks: The generalized exponential random graph model. PloS one, 7(1):e30136, 2012.
- Claire Donnat and Susan Holmes. Tracking network dynamics: A survey of distances and similarity metrics. arXiv preprint arXiv:1801.07351, 2018.
- Nathan Eagle et al. Reality mining: sensing complex social systems. Personal and ubiquitous computing, 10(4):255–268, 2006.
- Ian Fellows and Mark Handcock. Removing phase transitions from gibbs measures. In Artificial intelligence and statistics, pages 289–297. PMLR, 2017.
- Ian E Fellows. Why (and when and how) contrastive divergence works. arXiv preprint arXiv:1405.0602, 2014.
- Ove Frank and David Strauss. Markov graphs. Journal of the American Statistical Association, 81(395):832–842, 1986.
- Valeria Gelardi, Jeanne Godard, Dany Paleressompulle, Nicolas Claidière, and Alain Barrat. Measuring social networks in primates: wearable sensors versus direct observations. Proceedings of the Royal Society A, 476(2236):20190737, 2020.
- Charles J Geyer and Elizabeth A Thompson. Constrained monte carlo maximum likelihood for dependent data. Journal of the Royal Statistical Society: Series B (Methodological), 54(3): 657–683, 1992.
- Ravi Goyal and Victor De Gruttola. Dynamic network prediction. Network Science, 8(4):574–595, 2020.

- Mark S Handcock, Garry Robins, Tom Snijders, Jim Moody, and Julian Besag. Assessing degeneracy in statistical models of social networks. Technical report, Working paper, 2003.
- Mark S. Handcock, David R. Hunter, Carter T. Butts, Steven M. Goodreau, Pavel N. Krivitsky, and Martina Morris. ergm: Fit, Simulate and Diagnose Exponential-Family Models for Networks. The Statnet Project (<https://statnet.org>), 2021. URL <https://CRAN.R-project.org/package=ergm>. R package version 4.1.2.
- Steve Hanneke and Eric P Xing. Discrete temporal models of social networks. In ICML workshop on Statistical Network Analysis, pages 115–125. Springer, 2006.
- Steve Hanneke, Wenjie Fu, and Eric P Xing. Discrete temporal models of social networks. Electronic Journal of Statistics, 4:585–605, 2010.
- Geoffrey E Hinton. Training products of experts by minimizing contrastive divergence. Neural Computation, 14(8):1771–1800, 2002.
- Paul W Holland and Samuel Leinhardt. An exponential family of probability distributions for directed graphs. Journal of the American Statistical Association, 76(373):33–50, 1981.
- Ruth M Hummel. Improving estimation for exponential-family random graph models. PhD thesis, The Pennsylvania State University, 2011.
- Ruth M Hummel, David R Hunter, and Mark S Handcock. Improving simulation-based algorithms for fitting ergms. Journal of Computational and Graphical Statistics, 21(4):920–939, 2012.
- David R Hunter and Mark S Handcock. Inference in curved exponential family models for networks. Journal of Computational and Graphical Statistics, 15(3):565–583, 2006.
- David R Hunter, Steven M Goodreau, and Mark S Handcock. Goodness of fit of social network models. Journal of the American Statistical Association, 103(481):248–258, 2008a.
- David R Hunter, Mark S Handcock, Carter T Butts, Steven M Goodreau, and Martina Morris. ergm: A package to fit, simulate and diagnose exponential-family models for networks. Journal of Statistical Software, 24(3):nihpa54860, 2008b.
- Binyan Jiang, Jailing Li, and Qiwei Yao. Autoregressive networks. arXiv preprint arXiv:2010.04492, 2020.
- Pavel N Krivitsky. Exponential-family random graph models for valued networks. Electronic Journal of Statistics, 6:1100, 2012.
- Pavel N Krivitsky. Using contrastive divergence to seed monte carlo mle for exponential-family random graph models. Computational Statistics & Data Analysis, 107:149–161, 2017.
- Pavel N. Krivitsky. ergm.count: Fit, Simulate and Diagnose Exponential-Family Models for Networks with Count Edges. The Statnet Project (<https://statnet.org>), 2019. URL <https://CRAN.R-project.org/package=ergm.count>. R package version 3.4.0.

- Pavel N Krivitsky and Mark S Handcock. A separable model for dynamic networks. Journal of the Royal Statistical Society. Series B, Statistical Methodology, 76(1):29, 2014.
- Pavel N Krivitsky, Mark S Handcock, and Martina Morris. Adjusting for network size and composition effects in exponential-family random graph models. Statistical Methodology, 8(4): 319–339, 2011.
- Steffen Lauritzen, Alessandro Rinaldo, and Kayvan Sadeghi. Random networks, graphical models and exchangeability. Journal of the Royal Statistical Society: Series B (Statistical Methodology), 80(3):481–508, 2018.
- Philip Leifeld and Skyler J Cranmer. A theoretical and empirical comparison of the temporal exponential random graph model and the stochastic actor-oriented model. Network Science, 7 (1):20–51, 2019.
- Jürgen Lerner, Natalie Indlekofer, Bobo Nick, and Ulrik Brandes. Conditional independence in dynamic networks. Journal of Mathematical Psychology, 57(6):275–283, 2013.
- Matthew Ludkin, Idris Eckley, and Peter Neal. Dynamic stochastic block models: parameter estimation and detection of changes in community structure. Statistics and Computing, 28(6): 1201–1213, 2018.
- Rossana Mastrandrea, Julie Fournet, and Alain Barrat. Contact patterns in a high school: a comparison between data collected using wearable sensors, contact diaries and friendship surveys. PloS one, 10(9):e0136497, 2015.
- Oscar Hernan Madrid Padilla, Yi Yu, and Carey E Priebe. Change point localization in dependent dynamic nonparametric random dot product graphs. arXiv preprint arXiv:1911.07494, 2019.
- Marianna Pensky. Dynamic network models and graphon estimation. The Annals of Statistics, 47 (4):2378–2403, 2019.
- Riccardo Rastelli, Pierre Latouche, and Nial Friel. Choosing the number of groups in a latent stochastic blockmodel for dynamic networks. Network Science, 6(4):469–493, 2018.
- Garry Robins and Philippa Pattison. Random graph models for temporal processes in social networks. Journal of Mathematical Sociology, 25(1):5–41, 2001.
- Daniel K Sewell and Yuguo Chen. Latent space models for dynamic networks with weighted edges. Social Networks, 44:105–116, 2016.
- Tom AB Snijders. The statistical evaluation of social network dynamics. Sociological Methodology, 31(1):361–395, 2001.
- Tom AB Snijders. Markov chain monte carlo estimation of exponential random graph models. Journal of Social Structure, 3(2):1–40, 2002.
- Tom AB Snijders. Models for longitudinal network data. Models and methods in social network analysis, 1:215–247, 2005.

- Tom AB Snijders, Philippa E Pattison, Garry L Robins, and Mark S Handcock. New specifications for exponential random graph models. *Sociological Methodology*, 36(1):99–153, 2006.
- Mohammed Suhail, Abhay Mittal, Behjat Siddiquie, Chris Broaddus, Jayan Eledath, Gerard Medioni, and Leonid Sigal. Energy-based learning for scene graph generation. *arXiv preprint arXiv:2103.02221*, 2021.
- Andrew C Thomas and Joseph K Blitzstein. Valued ties tell fewer lies: Why not to dichotomize network edges with thresholds. *arXiv preprint arXiv:1101.0788*, 2011.
- Medha Uppala and Mark S Handcock. Modeling wildfire ignition origins in southern california using linear network point processes. *The Annals of Applied Statistics*, 14(1):339–356, 2020.
- Philippe Vanhems, Alain Barrat, Ciro Cattuto, Jean-François Pinton, Nagham Khanafer, Corinne Régis, Byeul-a Kim, Brigitte Comte, and Nicolas Voirin. Estimating potential infection transmission routes in hospital wards using wearable proximity sensors. *PloS one*, 8(9):e73970, 2013.
- YX Rachel Wang, Lexin Li, Jingyi Jessica Li, and Haiyan Huang. Network modeling in biology: statistical methods for gene and brain networks. *Statistical Science*, 36(1):89–108, 2021.
- Stanley Wasserman and Philippa Pattison. Logit models and logistic regressions for social networks: I. an introduction to markov graphs andp. *Psychometrika*, 61(3):401–425, 1996.
- Danny Wyatt, Tanzeem Choudhury, and Jeff Bilmes. Dynamic multi-valued network models for predicting face-to-face conversations. In *NIPS workshop on Analyzing Networks and Learning with Graphs*. Citeseer, 2009.
- Danny Wyatt, Tanzeem Choudhury, and Jeff Bilmes. Discovering long range properties of social networks with multi-valued time-inhomogeneous models. In *Proceedings of the AAAI Conference on Artificial Intelligence*, volume 24, 2010.
- Jian Xie, Youyi Bi, Zhenghui Sha, Mingxian Wang, Yan Fu, Noshir Contractor, Lin Gong, and Wei Chen. Data-driven dynamic network modeling for analyzing the evolution of product competitions. *Journal of Mechanical Design*, 142(3), 2020.
- George G Vega Yon, Andrew Slaughter, and Kayla de la Haye. Exponential random graph models for little networks. *Social Networks*, 64:225–238, 2021.
- Yi Yu, Oscar Hernan Madrid Padilla, Daren Wang, and Alessandro Rinaldo. Optimal network online change point localisation. *arXiv preprint arXiv:2101.05477*, 2021.
- Chen Zhang, Xinghua Dang, Tao Peng, and Chaokai Xue. Dynamic evolution of venture capital network in clean energy industries based on stergm. *Sustainability*, 11(22):6313, 2019.